World Journal of Radiology

Submit a Manuscript: https://www.f6publishing.com

World J Radiol 2021 September 28; 13(9): 258-282

DOI: 10.4329/wjr.v13.i9.258

ISSN 1949-8470 (online)

REVIEW

Comprehensive literature review on the radiographic findings, imaging modalities, and the role of radiology in the COVID-19 pandemic

Aman Pal, Abulhassan Ali, Timothy R Young, Juan Oostenbrink, Akul Prabhakar, Amogh Prabhakar, Nina Deacon, Amar Arnold, Ahmed Eltayeb, Charles Yap, David M Young, Alan Tang, Subramanian Lakshmanan, Ying Yi Lim, Martha Pokarowski, Pramath Kakodkar

ORCID number: Aman Pal 0000-0001-7834-918X; Abulhassan Ali 0000-0001-7246-8444; Timothy R Young 0000-0001-8444-8571; Juan Oostenbrink 0000-0003-0103-4678; Akul Prabhakar 0000-0002-5451-8425; Amogh Prabhakar 0000-0001-9664-1520; Nina Deacon 0000-0002-8580-9081; Amar Arnold 0000-0002-8624-2996; Ahmed Eltayeb 0000-0002-3772-3179; Charles Yap 0000-0001-9477-6827; David M Young 0000-0001-6551-7527; Alan Tang 0000-0001-5744-3628; Subramanian Lakshmanan 0000-0002-2070-3657; Ying Yi Lim 0000-0003-1528-0191; Martha Pokarowski 0000-0001-6647-7029; Pramath Kakodkar 0000-0002-5288-1247.

Author contributions: Pal A, Ali A, Young TR, Oostenbrink J, Prabhakar A, Prabhakar A, Deacon N, Arnold A, Yap C, Young DM, Tang A, Lakshmanan S, and Kakodkar P performed acquisition and curation of the data; Pal A, Ali A, Young TR and Kakodkar P analyzed the data; Pal A, Ali A, Oostenbrink J, Prabhakar A, Prabhakar A, Deacon N, Arnold A, Eltayeb A, Eltayeb A, Yap C, Young DM, Tang A, and Kakodkar P performed interpretation of the data; Pal A, Ali A, Young TR, Oostenbrink J, Prabhakar A,

Aman Pal, Abulhassan Ali, Timothy R Young, Juan Oostenbrink, Akul Prabhakar, Amogh Prabhakar, Nina Deacon, Amar Arnold, Ahmed Eltayeb, Charles Yap, Subramanian Lakshmanan, Ying Yi Lim, Pramath Kakodkar, School of Medicine, National University of Ireland Galway, Galway H91 TK33, Galway, Ireland

David M Young, Department of Computer Science, Yale University, New Haven, CO 06520, United States

Alan Tang, Department of Health Science, Duke University, Durham, NC 27708, United States

Martha Pokarowski, The Hospital for Sick Kids, University of Toronto, Toronto M5S, Ontario, Canada

Corresponding author: Pramath Kakodkar, MD, Doctor, School of Medicine, National University of Ireland Galway, University Road, Galway H91 TK33, Galway, Ireland.
p.kakodkar1@nuigalway.ie

Abstract

Since the outbreak of the coronavirus disease 2019 (COVID-19) pandemic, over 103214008 cases have been reported, with more than 2231158 deaths as of January 31, 2021. Although the gold standard for diagnosis of this disease remains the reverse-transcription polymerase chain reaction of nasopharyngeal and oropharyngeal swabs, its false-negative rates have ignited the use of medical imaging as an important adjunct or alternative. Medical imaging assists in identifying the pathogenesis, the degree of pulmonary damage, and the characteristic features in each imaging modality. This literature review collates the characteristic radiographic findings of COVID-19 in various imaging modalities while keeping the preliminary focus on chest radiography, computed tomography (CT), and ultrasound scans. Given the higher sensitivity and greater proficiency in detecting characteristic findings during the early stages, CT scans are more reliable in diagnosis and serve as a practical method in following up the disease time course. As research rapidly expands, we have emphasized the CO-RADS classification system as a tool to aid in communicating the likelihood of COVID-19 suspicion among healthcare workers. Additionally, the utilization of other scoring

Prabhakar A, Deacon N, Arnold A, Eltayeb A, Yap C, Young DM, Tang A, Lakshmanan S, Lim YY, Pokarowski M, and Kakodkar P wrote the original draft; Pal A, Lim YY, Pokarowski M, and Kakodkar P performed the critical revision; All authors have read and approved the final manuscript.

Conflict-of-interest statement: Authors declare no conflict of interest for this article.

Manuscript source: Invited manuscript

Specialty type: Radiology, nuclear medicine and medical imaging

Country/Territory of origin: Ireland

Peer-review report's scientific quality classification

Grade A (Excellent): 0
Grade B (Very good): 0
Grade C (Good): C
Grade D (Fair): 0
Grade E (Poor): 0

Received: February 6, 2021
Peer-review started: February 6, 2021
First decision: March 17, 2021
Revised: March 28, 2021
Accepted: August 4, 2021
Article in press: August 4, 2021
Published online: September 28, 2021

P-Reviewer: Kashyap MK
S-Editor: Liu M
L-Editor: Filipodia
P-Editor: Liu JH

systems such as MuLBSTA, Radiological Assessment of Lung Edema, and Brixia in this pandemic are reviewed as they integrate the radiographic findings into an objective scoring system to risk stratify the patients and predict the severity of disease. Furthermore, current progress in the utilization of artificial intelligence *via* radiomics is evaluated. Lastly, the lesson from the first wave and preparation for the second wave from the point of view of radiology are summarized.

Key Words: Coronavirus; COVID-19; Computed tomography; Ultrasound; MuLBSTA Scoring system; Radiological Assessment of Lung Edema classification; Brixia score

Core Tip: Since there is a rapid expansion and knowledge regarding the radiological findings in coronavirus disease 2019 (COVID-19), it is important to condense and collate the most important findings into a one-stop guide. We tried to undertake the same and provide digital images with markings that would be helpful for anyone interested in understanding the typical radiological features alongside the evidence-based findings of COVID-19 pneumonia. Additionally, we highlight and provide evidence-based findings regarding the predominantly utilized clinical scoring systems that integrate radiology.

Citation: Pal A, Ali A, Young TR, Oostenbrink J, Prabhakar A, Prabhakar A, Deacon N, Arnold A, Eltayeb A, Yap C, Young DM, Tang A, Lakshmanan S, Lim YY, Pokarowski M, Kakodkar P. Comprehensive literature review on the radiographic findings, imaging modalities, and the role of radiology in the COVID-19 pandemic. *World J Radiol* 2021; 13(9): 258-282
URL: https://www.wjgnet.com/1949-8470/full/v13/i9/258.htm
DOI: https://dx.doi.org/10.4329/wjr.v13.i9.258

INTRODUCTION

The current standard for the definitive diagnosis of coronavirus disease 2019 (COVID-19) is reverse-transcription polymerase chain reaction (RT-PCR) from the upper respiratory tract *via* nasopharyngeal and oropharyngeal swabs[1]. The diagnostic accuracy of real-time RT-PCR is as high as 95%[2]. However, the limitations of RT-PCR lies in its much lower diagnostic accuracy; it has high specificity but variable sensitivity ranging from 60%-70% to 95%-97%, respectively[3-5].

Medical imaging plays a key role in assisting the clinical decisions made towards the diagnosis, management, and follow-up of COVID-19 patients. This review presents the current literature related to the characteristics and key findings of COVID-19 in common radiological imaging modalities such as chest x-rays (CXRs), computed tomography (CT), and lung ultrasonography (LUS). To objectively stratify the severity of COVID-19, CXRs and CT scans are used in conjunction with various classifications systems such as CO-RADS, MuLBSTA, and the Radiological Assessment of Lung Edema (RALE) to facilitate the appropriate evaluation and treatment for infected cases. These are also explored within this review. Other imaging modalities such as magnetic resonance imaging (MRI), positron emission tomography (PET), and echocardiography are less commonly used but can be ordered to assess certain complications and treatment responses. Prior to reviewing these topics, the fundamental basics of COVID-19 pathophysiology are highlighted in the following section.

Pathophysiology of COVID-19

Aerosolization of respiratory droplets containing the severe acute respiratory syndrome coronavirus-2 (SARS-CoV-2) is the primary mode of transmission of COVID-19. The SARS-CoV-2 virion can further inoculate the mucous membranes *via* the facial T-zone (eyes, nose, and mouth). The current suggested model of pathogenesis for SARS-CoV-2 infection is composed of three phases: Viral replication, hyperactive immune system, and pulmonary destruction[6]. These phases are discussed in the following subsections.

Viral replication

Viral particles manifest their infectivity through replication within the host cell in the following five steps: Attachment, penetration, biosynthesis, maturation, and release [7]. SARS-CoV-2 binds with high affinity to angiotensin-converting enzyme 2 (ACE2) receptors and transmembrane protease serine 2 (TMPRSS2) receptors. Interestingly the ACE2 receptors are predominantly expressed with high density within the type II pneumocytes of the lung[8]. These receptors are also found in the heart (pericytes), ileum (enterocytes), kidney (podocytes), and bladder (urothelial cells)[8]. Once SARS-CoV-2 attaches to host receptors (ACE2 and TMPRSS2), the virion fuses with the membrane and enters the cell *via* endocytosis. Subsequently, inside the cell, the viral RNA enters the nucleus and alters the replication machinery to biosynthesize viral proteins. Upon maturation of the new viral particles, they are released to infect and continue their vicious cycle in other nearby cells[7].

Hyperactive immune system

Immune hyperactivity is a result of the stress-induced apoptosis of the affected cells and the viral RNA being recognized as a foreign genome by Toll-like receptors[9]. This leads to a cytokine storm (release of tumor necrosis factor, interleukin 6 [IL-6], IL-1β,

C-C motif chemokine ligand 2), which is stimulated by macrophages and dendritic cells and causes the infiltration of several inflammatory mediators in the alveolar-capillary interface[9]. Since there is a high density of ACE2 receptors along the peripheries of the lung parenchyma, the majority of damage early on is seen at these sites as a characteristic pulmonary ground-glass opacity (GGO) detected by a CT scan.

Pulmonary destruction

Although the purpose of inflammatory mediators is to fight against the virus until development of the adaptive immune system, their excessive infiltration damages this membrane, causing a build-up of fluid within the alveolar sacs and lung injury that further reduces ventilation[10]. The migration of fluid into the alveolar sacs is governed by the imbalance in Starling forces; $F = k([P_c - P_a] - s[\pi_c - \pi_a])$[11]. The diffuse alveolar damage caused by the viral particles results in an increased capillary wall permeability (high k value), thereby increasing the force at which fluid migrates from the capillaries to the alveolar space. Figure 1 summarizes the findings of Gralinski *et al* [12] as an illustration of the progressive development within an infected alveolus, both pathologically and radiologically[12]. The normal alveolar wall is comprised of type I and II pneumocytes, while the alveolar macrophages and surfactant reside in the alveolar space. In an acute setting of infection, the pneumocytes secrete inflammatory cytokines and exhibit cytopathic effects, while surfactant levels decrease. As the disease progresses, ventilation is impeded as pulmonary edema and airway debris coincide within the alveolar spaces, alongside the formation of hyaline membrane. Radiologically, the initial features of localized pulmonary edema is seen as GGOs (highly attenuated patches on CXR/CT) and as the severity of tissue damage increases, the pulmonary edema becomes more diffuse and is seen as wide areas of consolidation on the chest imaging modalities[13].

The radiodensities vary between each material and can be quantified using the Hounsfield scale, measured as Hounsfield units. Air, lung, ground glass, water, consolidation, and metal have radiodensities of -1000, -900, -800 to -100, 0, 30, and > 100, respectively[14]. The varying radiodensity of ground glass is associated with the severity of tissue damage and pulmonary edema as a more severe alveolar damage would elicit a higher radiodensity due to a greater fluid accumulation. Extreme tissue damage with complete alveolar consolidation presents as increased attenuation with anomalous opacities on chest imaging.

CHEST RADIOGRAPHY AND CT IMAGING

The role of imaging during the COVID-19 pandemic has yet to be fully explored. CXR and chest CT scans are not an official primary component of diagnosis but rather a supporting feature for diagnosis specifically to determine severity and the appropriate treatment response required. The high rate of false-negative results and fear of viral spread during sample transfers in RT-PCRs show the need for a systematic approach in the diagnosis of COVID-19 through a combination of clinical signs and radiological findings on CXR and CT, which are important in determining the severity of disease and guiding treatment responses[15]. It is important to note that chest CTs have the additional advantage of detecting changes of COVID-19 pneumonia in asymptomatic

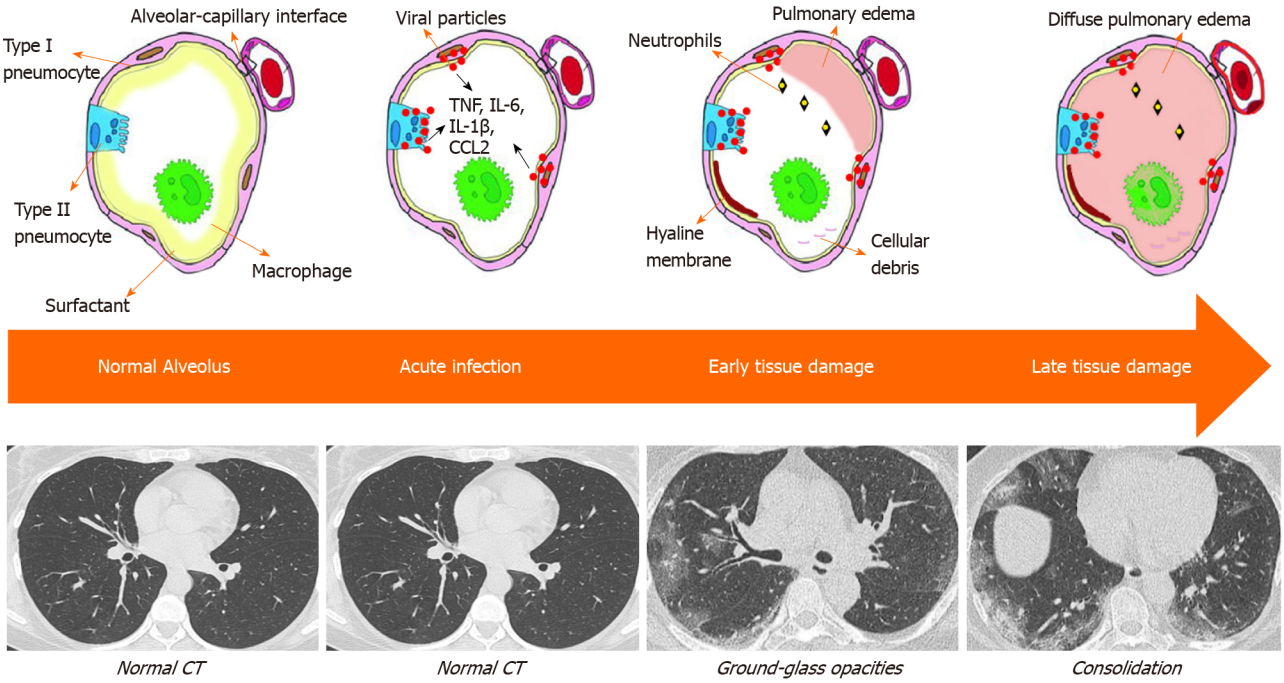

Figure 1 Model of infected lung through pathological and radiological perspectives.

patients[16].

CLASSICAL FINDINGS IN CHEST RADIOGRAPHY

Admitted in-patients presenting with COVID-19 provide a large repository of radiological images due to the ease of evaluations *via* solitary portable CXR. Findings of COVID-19 on CXR include hazy opacification, which is the radiographic equivalent to GGO found on a chest CT scan. These hazy opacifications have a predilection for the basal lung and its peripheries. These opacifications may be unilateral or bilateral. In severe cases, the middle to upper fields of the lung may become affected. In the penultimate disease stage (days 10-12), the areas of opacity coalesce and become denser. This presents as patchy consolidates similar to the pattern of acute respiratory distress syndrome (ARDS)[13]. The compilation of diagnostic factors such as signs, symptoms, oxygen saturation, and CXR appearance can offer a faster and inexpensive method for severity assessment. Most notable CXR findings included bilateral chest involvement 76.8% (95% confidence interval [CI]: 62.5%-87%), consolidation 75.5% (95%CI: 50.5%-91%), GGO 71% (95%CI: 40%-90%), and unilateral chest involvement in 16.5% (95%CI: 8.5%-29.5%)[17]. Some less common CXR findings include reticular interstitial thickening in 39.9% (n = 107/268), nodules 9.3% (n = 25/268), and pneumothorax, or pleural effusion (1%-3%)[18]. These findings could be a consequence of COVID-19 or pre-existing comorbidities, or just coincidental. Figure 2 shows a collection of chest radiographs with abnormal findings with a background of a positive SARS-CoV-2 PCR test. Examples of bilateral patchiness (Figure 2A), unilateral GGO (Figure 2B), pneumothorax (Figure 2C), and linear patchiness (Figure 2D) are modified from Singh *et al*[15], Martini *et al*[19], Rampa *et al*[20], and Kaufman *et al*[21]. Examples of nodular (Figure 2E) and reticular consolidations (Figure 2F) are modified from Yasin *et al*[22].

One large study (n = 1198) showed that the sensitivity and specificity of CXR for detecting features of COVID-19 pneumonia were 56% (95%CI: 51%-60%) and 60% (95%CI: 54%-65%), respectively[23]. In comparison, the chest CT provides an increase in sensitivity by 29% (95%CI: 19%-38%) in comparison to CXR[23]. This variable explains the limited usage of CXR in the screening, diagnosis, or follow-up of COVID-19 patients.

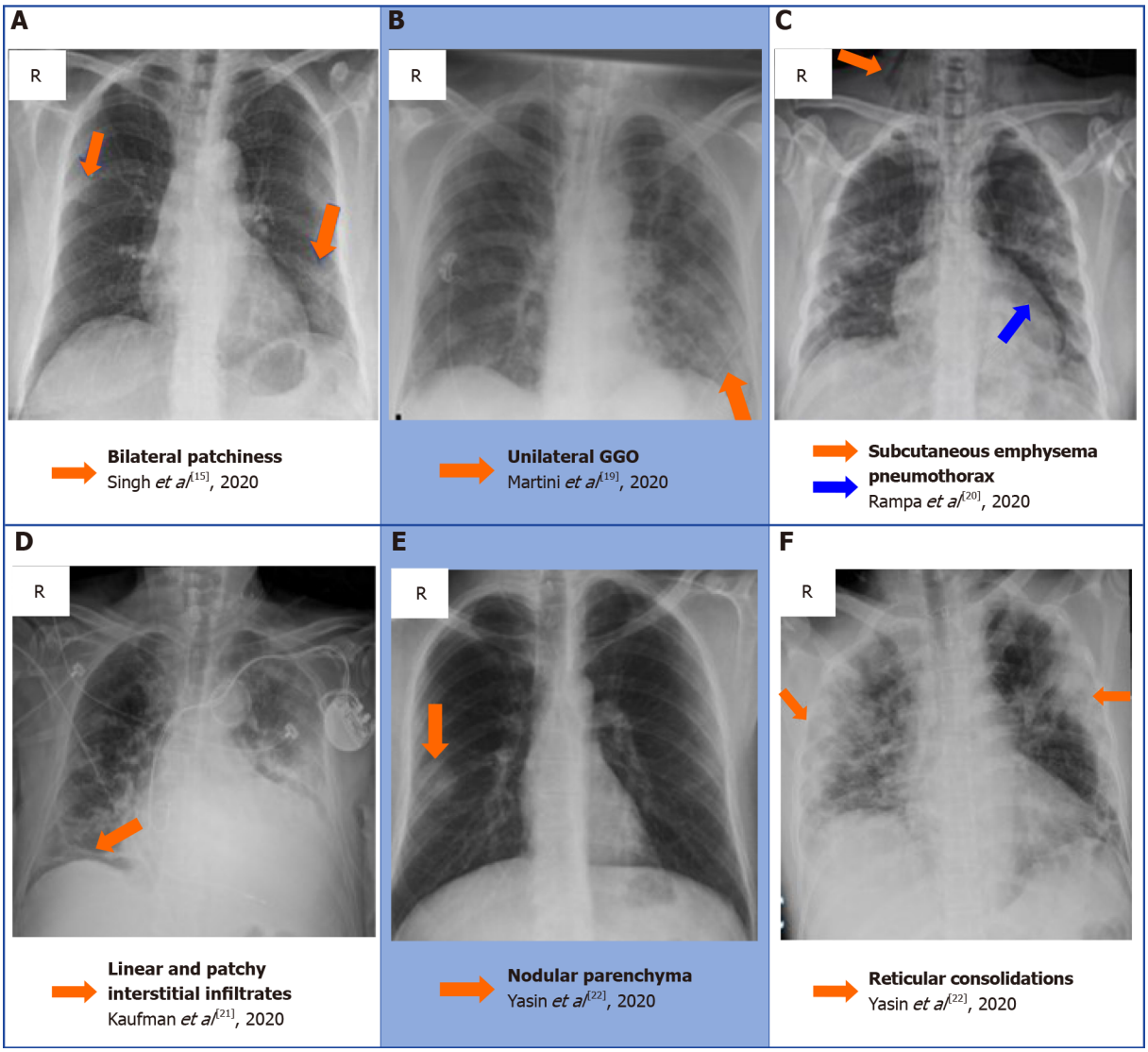

Figure 2 A collection of chest radiographs that displays some of the common and rare findings of coronavirus disease 2019 pneumonia [15,19-22]. A: Bilateral patchiness; B: Unilateral ground glass opacification; C: Subcutaneous emphysema secondary to a pneumothorax; D: Linear and patchy interstitial infiltrate in the right basal zone; E: Nodular appearance of the right lobe parenchyma; F: reticular appearance of the consolidation bilaterally. A: Citation: Singh B, Kaur P, Reid RJ, Shamoon F, Bikkina M. COVID-19 and Influenza Co-Infection: Report of Three Cases. *Cureus* 2020; 12: e9852. Copyright ©The Author(s) 2020. Published by Cureus; B: Citation: Martini K, Blüthgen C, Walter JE, Messerli M, Nguyen-Kim TD, Frauenfelder T. Accuracy of Conventional and Machine Learning Enhanced Chest Radiography for the Assessment of COVID-19 Pneumonia: Intra-Individual Comparison with CT. *Journal of Clinical Medicine* 2020;.9: 3576 Copyright ©The Author(s) 2020. Published by MDPI, Basel, Switzerland; C: Citation: Rampa L, Miceli A, Casilli F, Biraghi T, Barbara B, Donatelli F. Lung complication in COVID-19 convalescence: A spontaneous pneumothorax and pneumatocele case report. *Journal of Respiratory Diseases and Medicine* 2020; 2. Copyright ©The Author(s) 2020. Published by Open-access article; D: Citation: Kaufman A, Naidu S, Ramachandran S, Kaufman D, Fayad Z, Mani V. Review of radiographic findings in COVID-19. *World Journal of Radiology* 2020; 12: 142-55. Copyright ©The Author(s) 2020. Published by Baishideng Publishing Group Inc; E and F: Citation: Yasin R, Gouda W. Chest X-ray findings monitoring COVID-19 disease course and severity. *The Egyptian Journal of Radiology and Nuclear Medicine* 2020; 51: 193. Copyright ©The Author(s) 2020. Published by BMJ.

CLASSICAL CT FINDINGS OF COVID-19 PNEUMONIA

While CXR is a practical method of screening, a recent meta-analysis showed that chest CTs are superior in the screening and assessment of COVID-19 pneumonia due to its increased sensitivity of 91.9% (95%CI: 89.8%-93.7%)[2]. CT is proficient in detecting early signs of COVID-19 pneumonia in comparison to CXR. This is evident by the detection of early-stage GGOs and consolidative opacities, which are often not visible on CXR or may appear normal with minimal interstitial markings[24]. In similar patients where CXR detects minimal interstitial markings, subtle opacities, or occult signs, CT would display identifiable GGO. Figure 3 shows a summary of the meta-analysis of classical and ancillary CT imaging findings by Bao *et al*[25].

Ancillary late-stage CT finding of COVID-19 pneumonia includes crazy-paving, which is defined by the Fleischner Society as diffuse GGO with superimposed

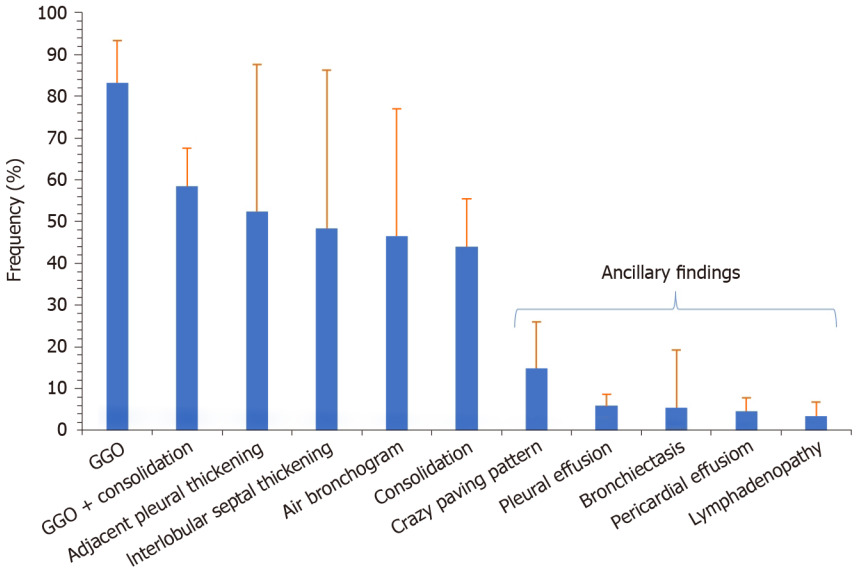

Figure 3 Summary of the frequency distribution of classical and ancillary computed tomography imaging findings in coronavirus disease 2019 pneumonia. The whiskers indicate the 95% confidence interval. GGO: Ground-glass opacity.

thickened intralobular lines and interlobular septa. The discovery of crazy-paving on a CT image is radiographic evidence of progressive COVID-19[26]. Additionally, diffuse patchy consolidation with reticular configuration becomes more predominant later in the disease course. Other classical chest CT findings that rule-in COVID-19 are lateralization of GGO early in the disease course, with multifocal, bilateral, and basilar lobe predominance, peripheral GGO with a rounded or oval morphology[18]. Figure 4 shows a collection of some notable classical chest CT findings in the axial plane of COVID-19 patients. Examples of classical findings such as GGOs (Figure 4A), air bronchograms (Figure 4B), bronchial thickening (Figure 4E), and pleural adhesions (Figure 4F) are all modified from Fu *et al*[27]. Additionally, examples of GGO superimposed with consolidation (Figure 4D) and crazy paving sign (Figure 4C) are modified from Gillespie *et al*[26] and Ali *et al*[28].

Additionally, Figure 5 shows the common lobes wherein classical CT findings of COVID-19 are distributed based on the findings of a meta-analysis by Bao *et al*[25]. Although the exact mechanism is unidentified, the increased incidence of findings in the lower lobes may be related to the anatomical structure of the trachea and bronchi, alongside the gravitational force that allows the virion particles to settle at the base more readily. Furthermore, since the right main bronchus bifurcates at a smaller angle and is wider than the left main bronchus, the virion particles can travel more easily towards the right lower lobe.

NON-CLASSICAL CT FINDINGS OF COVID-19 PNEUMONIA

Less commonly reported imaging findings that may help to rule-in COVID-19 is subsegmental vascular engorgement[29]. Furthermore, another uncommon but positive feature that rules in COVID-19 is the atoll sign on CT, also referred to as the reverse halo sign[18]. This is defined as a focal rounded area of GGO which is surrounded by a complete or nearly complete ring of denser consolidation which is observed on CT[30]. Other causes of the reverse-halo sign may be chronic lung injury, and notably, may raise the concern of pulmonary infarction. Interestingly, one meta-analysis indicates that these non-classical CT findings might be more common than previously predicted. Figure 6 shows the summary of results from a meta-analysis conducted by Ojha *et al*[31] to tabulate the incidence of non-classical CT findings in COVID-19 patients.

Figure 7 displays a collection of chest CTs in the axial plane that are examples of the ancillary findings in COVID-19. Examples of vascular enlargement (Figure 7A) are modified from Kwee *et al*[32]. Examples of subpleural curvilinear opacities (Figure 7B) and reverse halo sign (Figure 7F) are modified from Kong *et al*[33]. Additionally, examples of reticular pattern (Figure 7C), pulmonary nodules (Figure 7D), and

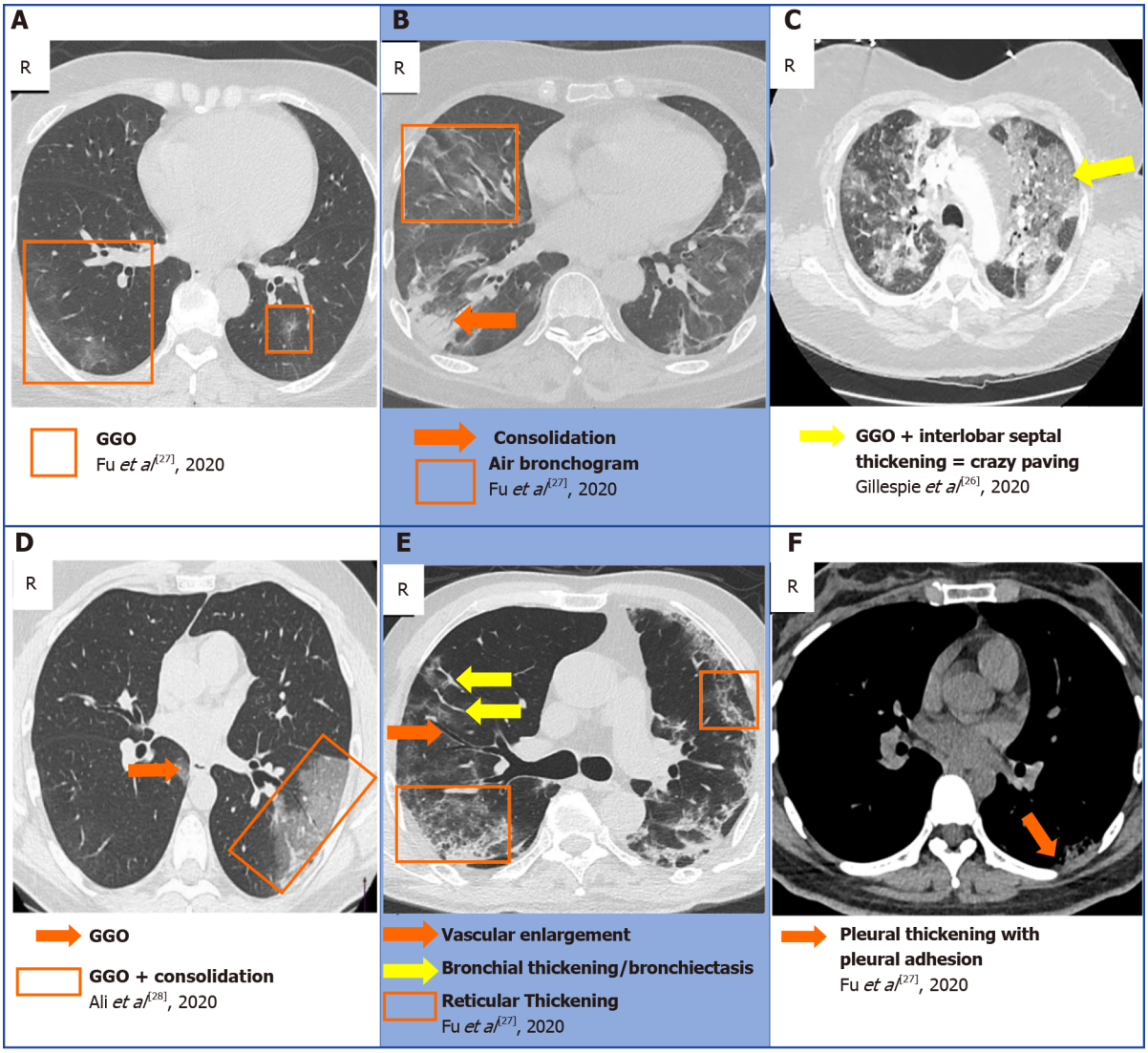

Figure 4 A collection of chest computed tomography that displays some of the classical findings of coronavirus disease 2019 pneumonia[26-28]. A: Ground-glass opacity (GGO); B: Consolidation and air bronchogram; C: Crazy paving; D: GGO superimposed with consolidation; E: Bronchiectasis, reticular thickening, with vascular enlargement; F: Pleural adhesion. A, B, E and F: Citation: Fu Z, Tang N, Chen Y, Ma L, Wei Y, Lu Y, Ye K, Liu H, Tang F, Huang G, Yang Y, Xu F. CT features of COVID-19 patients with two consecutive negative RT-PCR tests after treatment. *Science Report* 2020; 10: 11548. Copyright ©The Author(s) 2020. Published by Springer Nature; C: Citation: Gillespie M, Flannery P, Schumann JA, Dincher N, Mills R, Can A. Crazy-Paving: A Computed Tomographic Finding of Coronavirus Disease 2019. *Clinical Practice and Cases in Emergency Medicine* 2020; 4: 461-463. Copyright ©The Author(s) 2020. Published by UC Irvine; D: Citation: Ali TF, Tawab MA, ElHariri MA. CT chest of COVID-19 patients: what should a radiologist know? *Egyptian Journal of Radiology and Nuclear Medicine* 2020; 51: 120. Copyright ©The Author(s) 2020. Published by Springer Nature.

bilateral hilar lymphadenopathy (Figure 7E) are modified from Meirelles *et al*[34], Zhang *et al*[35], Mughal *et al*[36], respectively.

Negative features that rule-out COVID-19 include lobar consolidation, which is more commonly seen in bacterial pneumonia rather than COVID-19 pneumonia, along with lack of GGO. Moreover, in early disease, there is a notable absence of features such as pleural effusion, mediastinal lymphadenopathy, lung cavitation and discrete pulmonary nodules such as the tree-in-bud sign in centrilobular nodules[24]. Ultimately, CT has an extremely high sensitivity of 94% in the detection of COVID-19; however, due to multiple pathologies which may be causative for the features seen in CT; CT has a particularly poor, and varying specificity of 25%-80%[37].

NON-COVID-19 CAUSES OF GGO

There are many causative pathologies unrelated to COVID-19, which may present as GGO on imaging, and this is the reason for the low specificity of CT imaging (25.1%, [95%CI: 21.0%-29.5%]) in diagnosing COVID-19 pneumonia[2]. Acute causes have

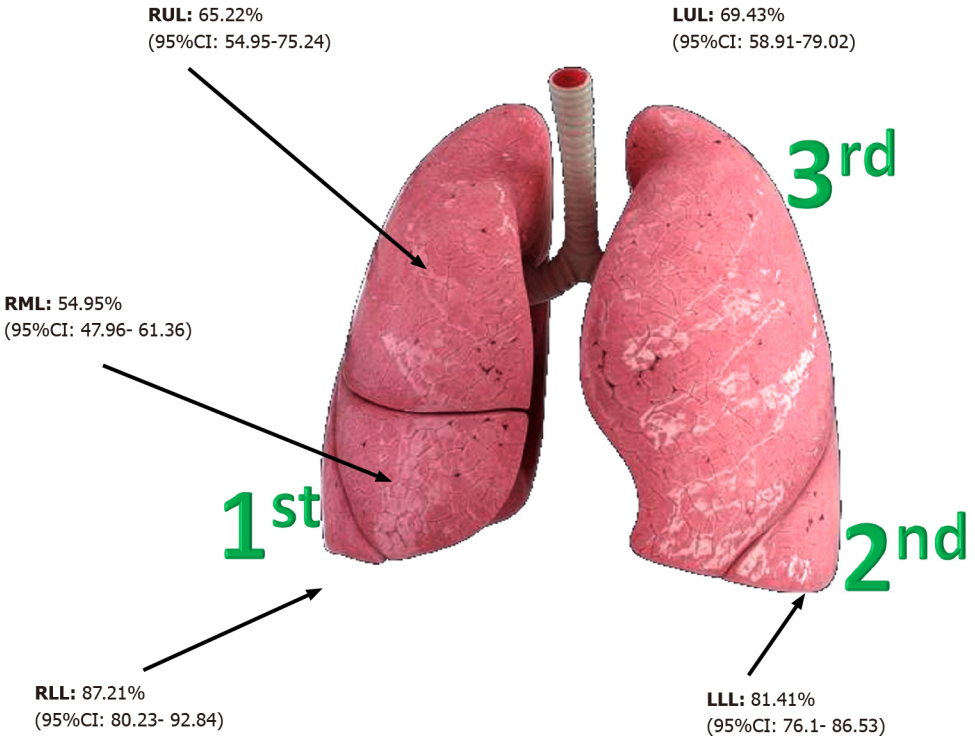

Figure 5 Summary of the frequency distribution of lesions in the lung lobes on computed tomography imaging of coronavirus disease 2019 patients. CI: Confidence interval; LLL: Left lower lobe; LUL: Left upper lobe (LUL); RLL: Right lower lobe; RML: Right middle lobe; RUL: Right upper lobe.

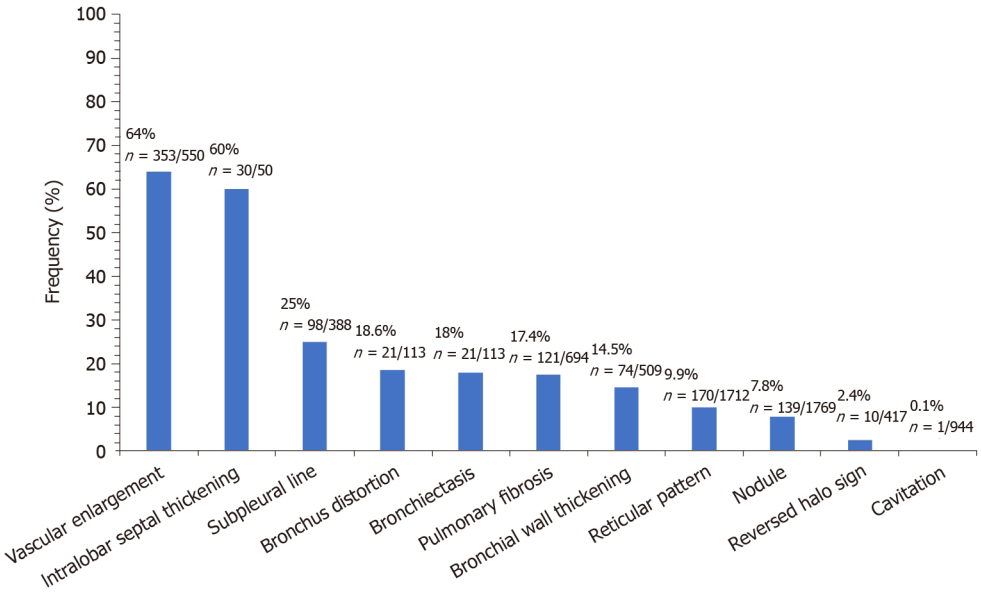

Figure 6 Summary of the frequency distribution of classical and ancillary computed tomography imaging findings in coronavirus disease 2019 pneumonia. The whiskers indicate the 95% confidence interval. The data are adapted from the meta-analysis conducted by Ojha *et al*[31].

abrupt signs on imaging arising in less than 4 wk. This may be pneumonia caused by a myriad of viruses such as influenza A or B, herpes simplex virus type 1, and cytomegalovirus[10]. In addition, acute eosinophilic pneumonia (AEP) may present as bilateral patchy GGO areas with interlobular septal thickening[38]. Drug toxicity due to cytotoxic drugs such as cyclophosphamide or bleomycin may manifest as scattered or diffuse areas of GGO[39]. Additional presentations may be due to chronic diseases lasting greater than 4 wk. Chronic eosinophilic pneumonia may also give rise to similar signs as AEP. Moreover, early lung cancer such as lung adenocarcinoma may be detected early by the appearance of GGO, improving surgical outcomes[40]. Ultimately, the varying causes of GGO on imaging demonstrates why CT alone is not

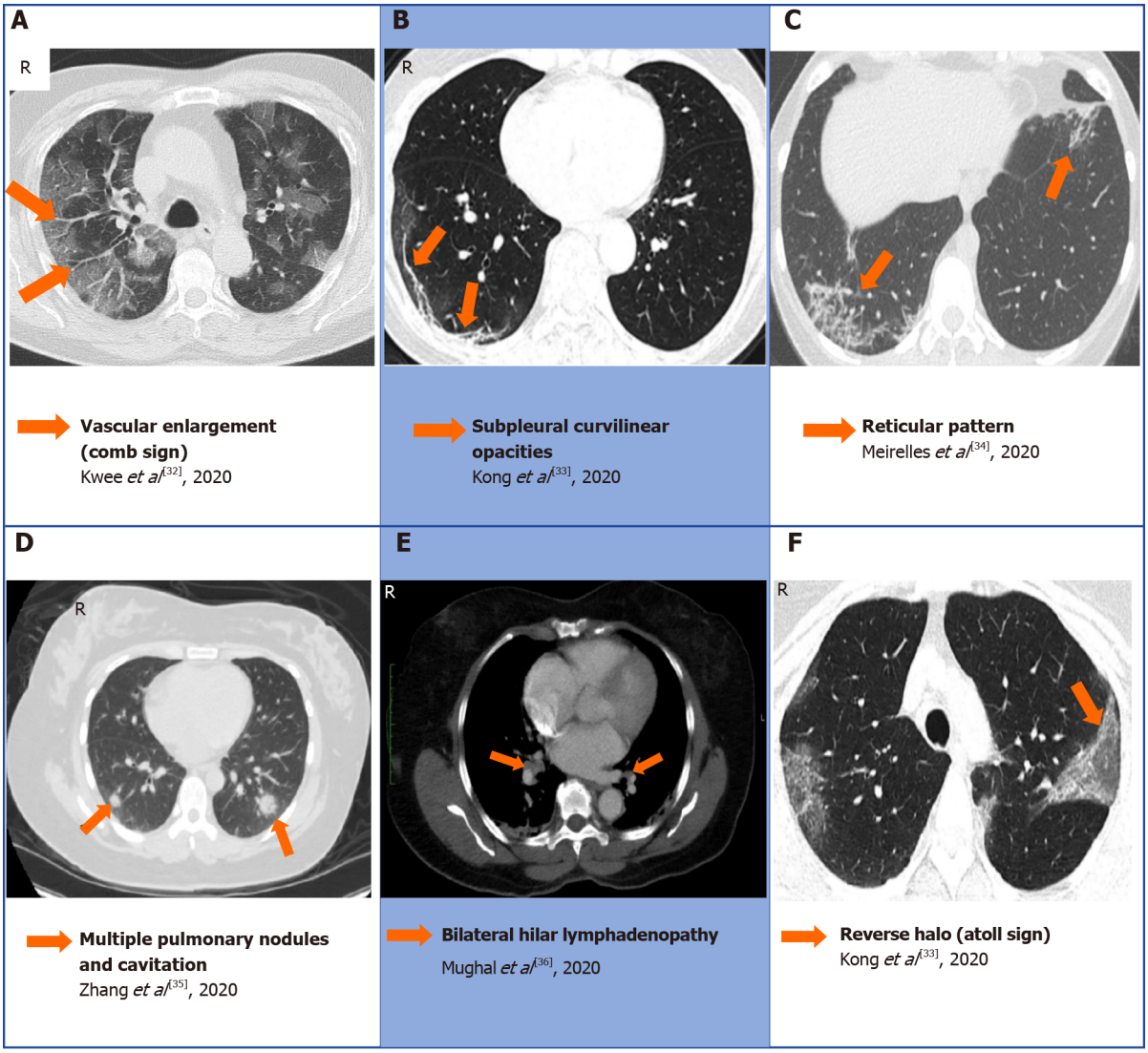

Figure 7 A collection of chest computed tomography that displays some of the atypical findings of coronavirus disease 2019 pneumonia [32-36]. A: Comb sign in the right lobe characterized by vascular enlargement; B: Curvilinear opacities in the subpleural area; C: Reticular pattern bilaterally; D: Multiple nodules and cavitation; E: Bilateral hilar lymphadenopathy; F: Atoll sign also known as reverse halo. A: Citation: Kwee TC, Kwee RM. Chest CT in COVID-19: What the radiologist needs to know. *Radiographics* 2020; 40: 1848-1865. Copyright ©The Author(s) 2021. Published by Radiographics; B and F: Citation: Kong W, Agarwal PP. Chest imaging appearance of COVID-19 infection. *Radiology: Cardiothoracic Imaging* 2020; 2: e200028. Copyright ©The Author(s) 2020. Published by the Radiological Society of North America, Inc; C: Citation: Meirelles GSP. COVID-19: A brief update for radiologists. *Radiologia Brasileira* 2020; 53: 320-328. Copyright ©The Author(s) 2020. Published by Radiology brasil; D: Citation: Zhang Q, Douglas A, Abideen ZU, Khanal S, Tzarnas S. Novel coronavirus (2019-nCoV) in disguise. *Cureus* 2020; 12: e7521. Copyright ©The Author(s) 2020. Published by Cureus; E: Citation: Mughal MS, Rehman R, Osman R, Kan N, Mirza H, Eng MH. Hilar lymphadenopathy, a novel finding in the setting of coronavirus disease (COVID-19): A case report. *Journal of Medical Case Reports* 2020; 14: 124. Copyright ©The Author(s) 2020. Published by BMC.

enough to accurately diagnose a patient with COVID-19 without clinical context, medication history, and RT-PCR/serology COVID-19 testing.

TIME COURSE: LAGGING OF COVID-19 FEATURES ON RADIOLOGICAL IMAGING

Although the preliminary imaging modality for patients presenting with COVID-19 is a solitary portable anteroposterior chest radiograph, many patients will have an early negative CXR/CT result. This can be due to a lack of macroscopic lung involvement at the time of presentation or minute findings on CXR/CT. During the early stages of disease (0-3 d), the viral particles take over host cell machinery, replicating and inducing a cytokine storm in the form of an acute infection. Gu *et al*[41] reported that nearly 13% of CT scans depict a normal finding in this early phase, while 63.2% of the cases exhibit a classical GGO appearance. A proposed hypothesis suggests that the

SARS-CoV-2 virion has not accumulated at an adequate density to induce pulmonary parenchymal damage. Therefore, the chest CT appears as a minimally hazy opacification with normal-appearing underlying vessels and bronchial structures. As the disease course progresses to the intermediate stage (4-7 d), there will be diffuse alveolar damage and GGO evolves into consolidation. The majority of the structures on chest CT will appear obscured in comparison to the primary GGO feature seen in the early stages. In the final stage (8-14 d), fibrotic lesions are significantly increased due to scarring of the lung tissue secondary to the resolution of organizing pneumonia [42]. Consolidation is also markedly enhanced in over 78% of the cases; however, the fibrotic lesions help distinguish the case presentation of late-stage from intermediate-stage disease in the majority of patients. Figure 8 summarizes the frequencies of typical CT findings (GGO, consolidation, fibrosis) based on the temporal stages of disease according to data from Gu *et al*[41].

ULTRASOUND IMAGING

LUS

LUS is an established imaging test for detecting various lung abnormalities, and in the context of COVID-19, may help clinicians with the diagnosis and evaluation of disease severity. Furthermore, it is useful for prognostic stratification and assessing the development of disease, and has assisted with the management of associated respiratory complications[43-46]. In comparison to CXR or CT, bedside LUS is faster, non-invasive, and radiation-free[47,48]. Point-of-care ultrasound (POCUS) machines are portable, allowing clinicians to assess patients at their bedside. This mitigates the need for patient mobilization to the radiology unit, thereby decreasing the risk of exposure to other patients[49,50]. POCUS is also economical, easy to learn, repeatable, and can obtain results of high reproducibility[51,52]. Moreover, POCUS offers an alternative imaging modality to triage patients' COVID risk levels and to streamline the pathway to warrant a requisition for second-level imaging or interventional management[51]. Heightened transmission of COVID-19 in healthcare workers has highlighted the importance of LUS in providing the option of concomitant execution of clinical examination and lung imaging at the bedside by the same physician[53,54].

CLASSICAL ULTRASOUND SIGNS: A AND B LINES

A- and B-lines are ultrasonographic artifacts that can be seen during the ultrasonography of an aerated lung. A-lines are typically horizontal artifacts that represent a normal lung surface[55]. B-lines are vertical, comet tail-like artifact indicating subpleural interstitial edema, likely representing reverberations generated by thickened interlobular septa and other subpleural structures[56]. In a normal lung ultrasound, the A-lines are horizontal to pleura and typical B-line patterns include a single cone-shaped line, single thin or thick line, or subpleural consolidation without air bronchogram[57].

ULTRASONOGRAPHIC PATTERNS IN COVID-19

Clear ultrasonographic patterns can be found in patients with COVID-19. Large numbers of B-lines, irregularity of the pleural line, and small clusters of subpleural pulmonary consolidations also frequently occur in the posterior and inferior areas[54,58]. Poggiali *et al*[44] concluded a strong correlation between LUS findings and concurrent CT scans in patients (n = 12) with COVID-19. These results also revealed diffuse B patterns and bilateral lung involvement with GGO in all of these patients [58]. Additionally, both imaging modalities also detected organizing pneumonia in four patients[59]. A summary of results from Norbedo *et al*[59] and McDermott *et al* [60] showed typical LUS findings in pediatric and adult patients with COVID-19. The literature review conducted by Norbedo *et al*[59] in pediatric patients (n = 18) with COVID-19 revealed LUS findings of B-line vertical artifacts, pleural irregularities, and small subpleural consolidations, as well as white patchy lung areas. A similar review conducted by Norbedo *et al*[59] on adult patients (n = 43) with COVID-19 revealed consistent LUS findings; irregular B-lines (focal), multifocal and confluent; thickening of pleural line with pleural line subpleural consolidations; and a variety of patterns

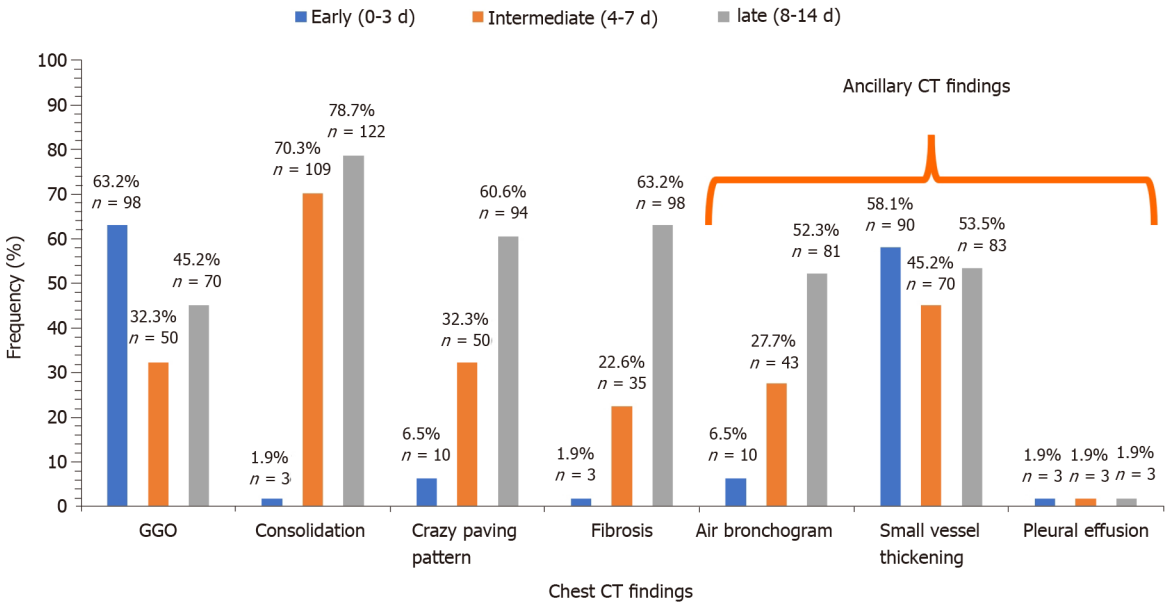

Figure 8 Summarizes the frequencies of chest classical and ancillary computed tomography findings at different stages of disease progression (early [*n* = 155], intermediate [*n* = 155], and late [*n* = 155]). Data acquired from Gu *et al*[41].

including multifocal small, non-translobar, and translobar with occasional mobile air bronchograms. The authors also concluded that pleural effusion in COVID-19 patients is uncommon[59].

LUS is able to detect dynamic changes associated with COVID-19. The main early-stage ultrasound finding was focal B-lines, which becomes multifocal and confluent as the disease progresses with further development of consolidations. During convalescence, B-lines and consolidations gradually disappear and are replaced by A-lines[57,61,62].

Interestingly, one study showed that LUS findings in patients with COVID-19 pneumonia exhibited typical patterns consistent with COVID-19 in 38.5% of cases (*n* = 52) and atypical patterns in 61.5% of cases (*n* = 83)[63]. The ability of LUS to diagnose COVID-19 can be inferred from its sensitivity of 76.9%, specificity of 77.1%, positive predictive value of 57.7%, and negative predictive value of 89.2%[63]. Additionally, when comparing LUS to chest CT, the results suggest a sensitivity and specificity of 65% and 72.7%, respectively[63]. Figure 9 shows a simplified flowchart for triaging patients presenting with respiratory symptoms during the COVID-19 pandemic in the emergency department as suggested by Schmid *et al*[63].

12-ZONE SCORING SYSTEM

In clinical practice, there are various scoring systems to quantify the extent of lung involvement, and in the context of COVID-19, we observed the most prominent one to be the 12-zone scoring system, used as a tool to assess regional and global lung aeration in ARDS as well as COVID-19 pneumonitis[61,64-66]. A total of 12 areas in the right and left lung are examined, namely the anterosuperior, anteroinferior, laterosuperior, lateroinferior, posterosuperior, and posteroinferior lung regions on each side of the lung. Scoring of each area is performed in accordance with the most severe lung ultrasound finding detected in the corresponding intercostal spaces and is given a score from 0-3, tallying up to a maximum of 36. Figure 10 outlines the assessed zone and the criteria for each of the values. The Australasian College of Emergency Medicine proposed a severity classification of patients based on this score as normal (0), mild (1-5), moderate (> 5-15), and severe (≥ 15)[65].

One study by Speidel *et al*[67] showed that the lung ultrasound scoring system (LUSS) had promising diagnostic efficacy with an odds ratio (OR) of 1.30, a 95%CI between 1.09 to 1.54 (P = 0.003), and an area under the curve (AUC) of 0.85 (95%CI: 0.71 to 0.99)[67]. Utilization of a cutoff of 8 of 36 points in participants (*n* = 10/11) with a primary diagnosis of COVID-19 were correctly predicted with a sensitivity of 91% (95%CI: 59% to 100%)[67]. In the cohort without a primary diagnosis of COVID-19

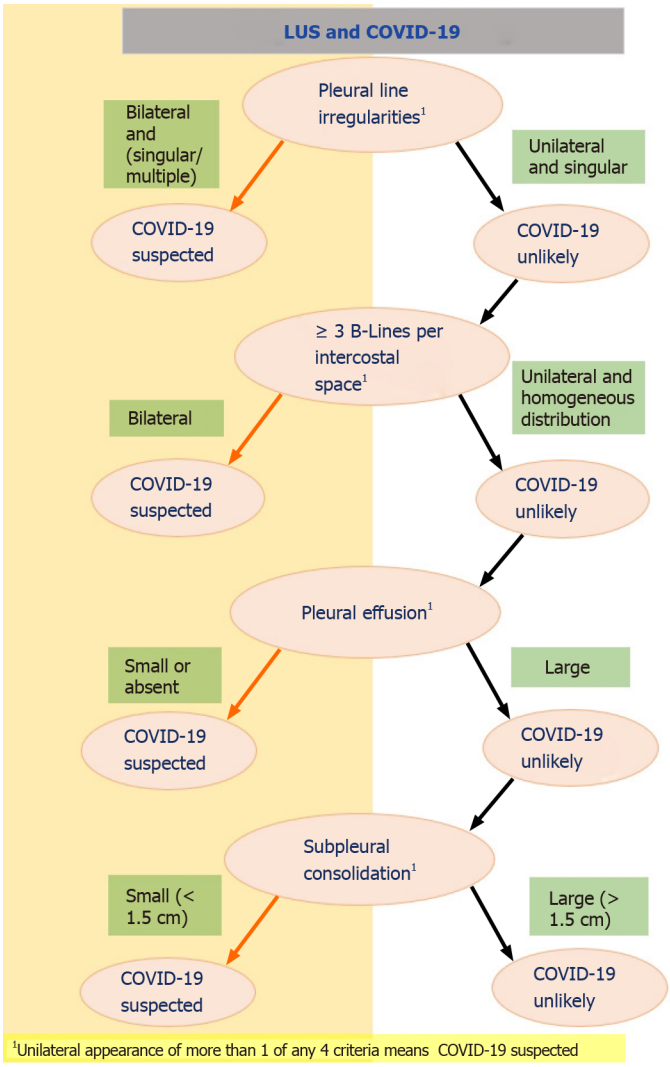

Figure 9 Shows a simplified flowchart guiding the triage in patients presenting with respiratory symptoms during the coronavirus disease 2019 pandemic using lung ultrasonography in the emergency department. [1]Unilateral appearance of more than 1 of any 4 criteria means coronavirus disease 2019 suspected. COVID-19: Coronavirus disease 2019; LUS: Lung ultrasonography.

(others, n = 38), COVID-19 was correctly ruled out in 29 of these 38 patients (specificity = 76%, 95%CI: 60% to 89%)[67]. LUSS, therefore, is a promising screening tool in hospitalized patients suspected of COVID-19. A summary of the results by Speidel *et al* [67] are shown in Figure 11 of typical LUS findings (B-line, and subpleural consolidations) and LUSS scores at varying lung zones in patients with and without a primary diagnosis of COVID-19.

LUS appears to have a promising role in screening clinically suspected or diagnosed COVID-19, only when it is implemented as an adjunct with other diagnostic modalities. An amalgamation of LUS findings with clinical history, physical examination, and knowledge of pretest probability will supplement increasing efficacy. POCUS may facilitate the physician in undertaking the appropriate management pathway or rule in an alternative diagnosis. The practicality of utilization of LUS will remain dependent on resource availability, personnel expertise, and flexibility of LUS configuration for each situation.

DISADVANTAGES OF LUS

LUS has been criticized for its low specificity in the diagnosis of COVID-19. This is because described features including confluent B-lines, consolidations, and irregular pleural lines simply refer to the lung surface density state and are not pathognomonic for COVID-19[68]. Additionally, LUS cannot detect deep lesions as the aerated parenchyma blocks the transmission of ultrasonography. In order for the lesion to

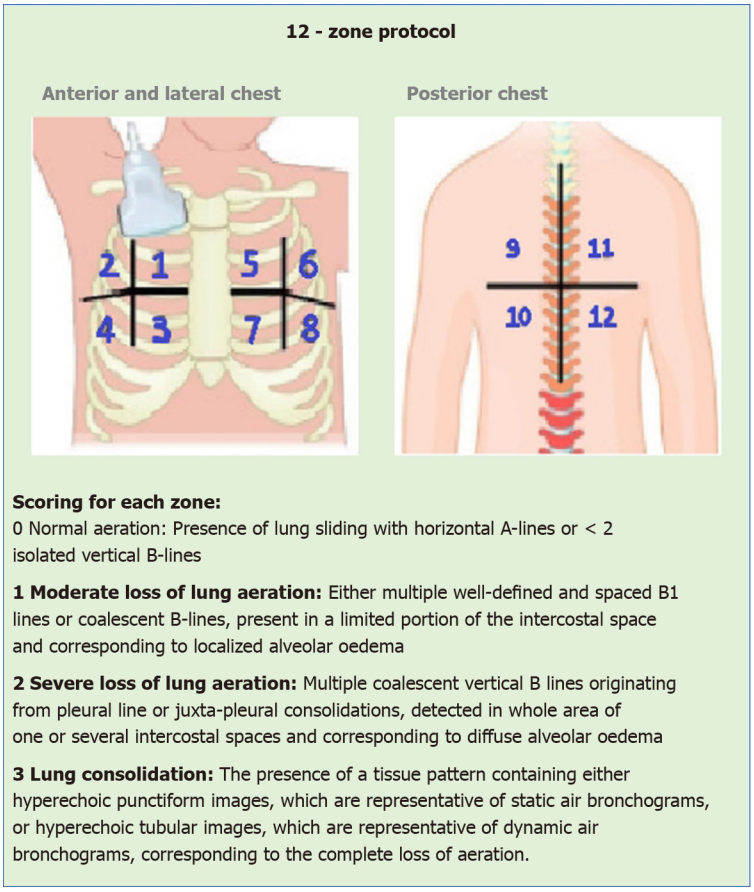

Figure 10 Schematic diagram describing the 12-zone assessed using the lung ultrasonography 12-zone scoring method. The criteria for each score value (0-3) is described and tabulated.

detected, it must extend to the pleural surface. Furthermore, LUS does not exclude COVID-19 in subjects with no pulmonary complications, and therefore cannot be used as a diagnostic tool by itself to stratify patients who may or may not be infected with COVID-19[47].

ROLE OF MRI, PET, AND ECHO IMAGING

There is no documented role of pulmonary MRI in the diagnosis of COVID-19 pneumonia. Cardiac MRIs may be helpful in the future to detect complications such as myocarditis and cardiomyopathy. Fluorodeoxyglucose PET (FDG-PET) scans are not used in emergencies, but some studies explain its utilization in describing the subtleties of typical pulmonary findings in COVID-19 pneumonia. The FDG-PET avidity corresponds to the GGOs in CTs, and this is because of the increased glucose requirement by the neutrophils at the site to fight the infection. There is a theoretical possibility of utilizing FDG-PET in the future to monitor treatment response, predict recovery and survey the long-term consequences of COVID-19.

Deep vein thrombosis and peripheral thrombosis are common in areas with high COVID-19 prevalence due to an increased risk of hypercoagulability; therefore, the use of compression ultrasonography is expected to increase. CT pulmonary angiography is mainly used to confirm the prognosis of pulmonary embolism (PE) and stratify patients with acute PE. Point of care echocardiography might be useful as the sensitivity of right ventricular dilation in detecting PE using POC echocardiography can be as high as 90%. Echocardiography can also be used to evaluate COVID-19-related acute cardiac injuries as abnormalities in echocardiography are linked to a worse prognosis and more severe disease[13].

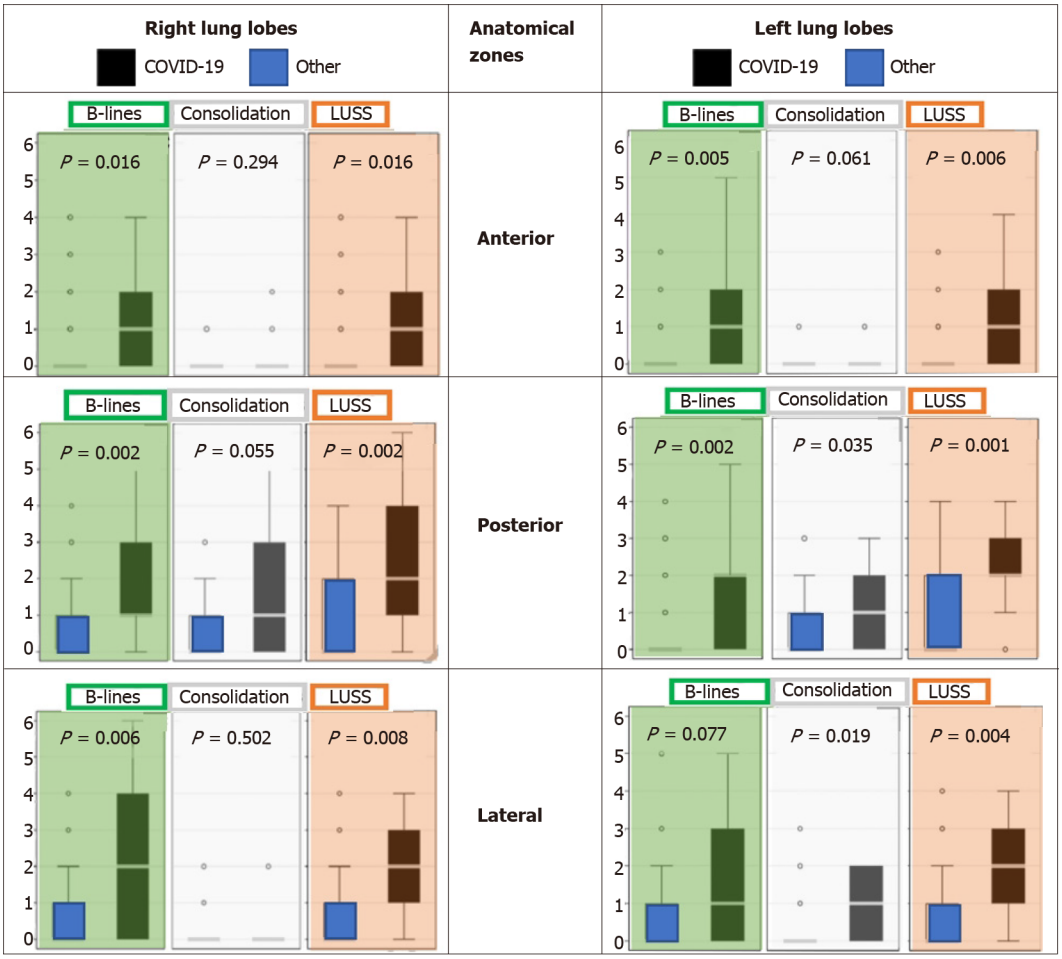

Figure 11 Lung ultrasonography presentation of B-lines (green panel), subpleural consolidations (white panel), and lung ultrasound scores (orange panel) at different lung zones (anterior, lateral, posterior) in patients with a primary diagnosis of coronavirus disease 2019 (*n* = 11) and without coronavirus disease 2019 (other, *n* = 38). Boxplots around median and interquartile range (IQR), with outliers within 1.5 IQR of the nearest quartile. Other (extrapulmonary infection/inflammation (*n* = 10), pneumonia of other etiology (*n* = 8), exacerbated asthma/ chronic obstructive pulmonary disease (*n* = 7), pulmonary neoplasia (*n* = 4), pulmonary embolism (*n* = 2), congestive heart failure (*n* = 2), and not documented (*n* = 5)). Statistically significant outcomes with $P < 0.05$. Data utilized from Speidel *et al*[67]. COVID-19: Coronavirus disease 2019; LUSS: Lung ultrasound score.

CLASSIFICATION SYSTEMS

CO-RADS classification system

In March 2020, a classification system by the Dutch Association for Radiology was implemented to aid with making the diagnosis of COVID-19. This system was called CO-RADS which stands for COVID-19 reporting and data system and was developed to report CT findings with ease and replicability among other physicians, as prior to this, no system had been developed directly for COVID-19. The system assigns the CT scan a CO-RAD score between 1 to 5 depending on the radiological findings of the chest, and in some cases, a score of 0 and 6 can be used. A score of 0 and 6 is used when the CT is uninterpretable, and a positive RT-PCR test must be present, respectively. Level 1 classification indicates a very low level of suspicion for COVID-19 as these cases do not have any nodules bilaterally and only have normal/benign findings[69]. Infections that can be considered level 1 for COVID-19 include mild or severe emphysema, perifissural nodules, lung tumor indications, and fibrosis[69]. This category is also known as negative for pneumonia. Level 2 is as having a low likelihood of COVID-19, but encompasses infectious diseases such as bronchitis, infectious bronchiolitis, bronchopneumonia, lobar pneumonia, and pulmonary abscesses[69]. CT features include those similar to an atypical pulmonary appearance like tree-in-bud sign, a centrilobular nodular pattern, lobar or segmental consolidation, and lung cavitation. Level 3 is the "middle ground" where the viewer can be unsure of the diagnosis as the features seen are those consistent with COVID-19 but also with viral pneumonia or non-infectious causes[69]. Findings in this level consist of perihilar GGO, homogenous extensive GGO with or without sparing of some secondary

pulmonary lobules, or GGO together with smooth interlobular septal thickening with or without pleural. GGO can also be seen on CT, which is characteristic of COVID-19, but the opacities seen are also compatible with organizing pneumonia. Although levels 4 and 5 have similar findings, the presence of GGO with or without consolidations in lung areas close to the visceral pleura indicates a CO-RADS score of level 5 [69]. A summary of the CO-RADS categories and its criteria outlined by Prokop *et al* are outlined in Table 1.

A study by Bellini *et al*[70] analyzed the diagnostic yield of CO-RADS in identifying lung involvement in patients suspected of COVID-19 (n = 572, COVID-19 (n = 142), not COVID-19 (n = 430)) by multiple radiologist and physicians at different levels of expertise. Overall, CO-RADS showed promising accuracy for lung involvement with a mean AUC of 72% (95%CI: 67% to 75%)[70]. The receiver operating characteristic (ROC) curve revealed that application of a threshold ≥ 4 resulted in a moderate specificity of 81% (95%CI: 76% to 84%) and a low sensitivity of 61% (95%CI: 52% to 69%)[70]. The CO-RADS rating among all readers was moderate as shown by Fleiss' Kappa statistic of 0.43 (95%CI: 0.42 to 0.44) and with a substantial agreement for categories; CO-RADS 1 (Fleiss' K = 0.61 (95%CI: 0.60 to 0.62) and for CO-RADS 5 (Fleiss' K = 0.60 (95%CI: 0.58 to 0.61))[70].

MULBSTA SCORING SYSTEM

Another scoring system used for COVID-19 is known as the MuLBSTA score, which looks at key components such as multi-lobar infiltration, hypo-lymphocytosis, bacterial coinfection, smoking history, hypertension, and age. Five points are assigned for multi-lobar infiltration, 4 points if the lymphocyte count is less than or equal to 0.8 × 10^9/L, 4 points for bacterial infiltration that is confirmed by lab results or on CT, 3 points for those who are currently smoking (2 for those who have previously been smokers), 2 points for hypertension, and 1 point for age above 60-years-old. A total score of 12 was used as the cut-off; those with scores between 0 and 11 were considered low risk while those with a score of ≥ 12 are considered high-risk patients. Those who are in the high-risk category are more likely to require intensive care unit treatment or were more likely to die due to the infection. This scoring system became useful as it helps to predict the prognosis of patients based on other clinical features and co-morbidities[66]. A retrospective study by Ma *et al*[71] (n = 330), showed that the ROC curve analysis on the MuLBSTA early warning scoring system for severe COVID-19 patients has an accuracy of 92.7% (95%CI: 89.2% to 96.3%), sensitivity of 65.1%, and specificity of 95.4%. These outcomes indicate that MuLBSTA is a good early warning system for severe COVID-19 patients.

RALE CLASSIFICATION

This system aims to associate the course and severity of CXR in COVID-19 with the diagnostic RT-PCR result. The RALE score involves individually assessing each lung and depending on how much of the lung is involved, a score is assigned to it. With no involvement, the score is 0, less than 25% lung involvement is 1, 25% lung involvement is 2, 50% of the lung is 3, and a level 4 classification is given when the lung is involved more than 75%. The overall score is calculated by adding the two scores, indicating the involvement of each lung[66]. The RALE score can be used to predict the outcomes of patients with COVID-19 pneumonia and their need for mechanical ventilation (MV). Interestingly, this scoring system is practical and only one of the few ones that incorporate a prognostic value. This makes it a valuable proxy system to compare against an artificial intelligence (AI) model.

One study by Ebrahimian *et al*[72] evaluated the implementation of AI such as the commercially available AI algorithm (qXR v2.1 c2; Qure.ai Technologies, Mumbai, Maharashtra) has been on the rise. This model was trained on patient data with a positive SARS-CoV-2 RT-PCR assay. The AI score had a strong positive correlation with RALE score for each site of the patient CXR (r^2 = 0.79 to 0.86; P < 0.0001)[72]. It also revealed that patients that received MV or deceased had a significantly higher AI or RALE score when compared to those not requiring MV or attained convalescence [72]. This study concluded that instead of comparing the RALE and AI score to the baseline CXRs, combining the RALE and AI score over progressive serial CXRs with clinical and lab data would drastically improve the predictability of both the AI score and the subjective RALE score.

Table 1 Association between CO-RADS categories and level of suspicion for pulmonary involvement of coronavirus disease 2019

CO-RADS category	Suspicion level for pulmonary involvement of COVID-19	Summary
0	Not interpretable	Scan insufficient for assigning score
1	Very low	Normal or non-infectious scan
2	Low	Typical for other infection but not COVID-19
3	Ambiguous	Non-specific features of COVID-19
4	High	Increased suspicion of COVID-19
5	Very high	Typical features of COVID-19
6	Proven	Positive RT-PCR test for COVID-19

Table modified from Prokop *et al*[69]. COVID-19: Coronavirus disease 2019.

BRIXIA SCORE

This score was designed and implemented for serial monitoring by the 'Radiology Unit 2 of ASST Spedali Civili di Brescia' and was later validated for risk stratification on a greater population by Borghesi *et al*[73]. According to this scoring system, the lung is divided into six different zones, three on each of the lungs, in either anteroposterior or posteroanterior views. With regards to the scoring of the zones, the score given can be between and including 0-3 based on the involvement of the lung. A score of 0 is given if there are no abnormalities seen on X-ray, a score of 1 is given when there are interstitial infiltrates. Two is given if there are interstitial and alveolar infiltrates, with the interstitial markings being more prominent. A score of 3 is assigned when there are both interstitial and alveolar infiltrates present, with the latter being more prominent. These scores are given to each of the 6 zones and are then aggregated to get a final score. This type of semiquantitative scoring makes CXR interpreting faster and more streamlined for evaluation[73]. The Brixia score becomes more useful when serial CXRs are performed as this enables documentation of additional sub-scores. The H-score is the highest Brixia score documented during the serial CXRs. Contrastingly, the L-score is the lowest Brixia score documented during the serial CXRs. Additionally, the Brixia score is documented at admission (A-score) and discharge/death (E-score).

One study by Maroldi *et al*[74] retrospectively assessed the clinical value of the Brixia score in 953 COVID-19 patients. In this study, the H-score was significantly higher with a median of 12 and interquartile range (IQR) between 9 to 14 in the deceased cohort compared to the discharged cohort (median: 8, IQR 5 to 11). Similarly, the L-score (7 *vs* 5; $P < 0.0003$), A-score (9 *vs* 8; $P < 0.039$), and E-score (12 *vs* 7; $P < 0.0001$) were all higher in the deceased cohort than the discharged cohort[74]. Overall, logistic regression showed a significant predictive value for H-score of OR 1.25. The ROC curve revealed an AUC of 0.863[74]. Additional Cox proportional hazards regression revealed age has a hazard ratio (HR) of 4.17 ($P = 0.0001$), H-score of < 9 has a HR 0.36 ($P = 0.0012$) and worsening of H-score compared to a score below 3, which has a HR of 1.57 ($P = 0.0227$) and is associated with a worse outcome[74]. These outcomes demonstrate the importance of the Brixia score in the monitoring and assessment of COVID-19 pneumonia and its strong correlation with a patient's prognosis.

PERMANENT LUNG SCARRING POST COVID-19

Research into the evolution of COVID-19 pneumonia imaging during the follow-up in the later stages of the disease is an interesting area. Zhao *et al*[75] demonstrated that at 3 mo, typical lung features (GGO, interstitial thickening. and crazy paving) were almost resolved, with some fibrosis. High-resolution CT scans of patients ($n = 55$) revealed that 67.27% had GGO ($n = 37$), 27.27% had interstitial thickening ($n = 15$), and 5.45% had crazy-paving patterns ($n = 3$)[75]. However, the study only included 55 patients who had non-critical COVID-19 pneumonia. Long-term follow-up studies with a larger sample size are crucial to better understand the trends in recovery. The available literature reports consistent findings of partial healing of GGO and consol-

idation from approximately day 14. In some patients, CT findings also demonstrated signs of fibrosis. In February to March 2020, a case series provided the earliest reports of follow-up CT findings. Partial healing of a mixed pattern of GGO and consolidation occurred from the day 14 onwards according to Duan and Qin[76], and Shi *et al*[77]. Wei *et al*[79], reported lung fibrosis in COVID-19 patients on day 12 which was corroborated by a case presented by Li *et al*[78] which described similar findings on day 14. Pan *et al*[80] presented a retrospective study (n = 63) following up COVID-19 patients. These patients were re-examined in intervals of 3-14 d wherein enlarged fibrous stripes and solid white nodules were documented. Pan *et al*[42] reported that after 14 d, 65% had GGO (n = 13/20) and 75% had consolidation (n = 15/20), but crazing-paving pattern was absent in all 20 patients. Bernheim *et al*[81] found that in 25 patients, after 6-12 d, 88% had GGO (n = 22/25) and 60% had consolidation (n = 15/25). Crazy-paving pattern was present in 20% of patients (n = 5), and 24% had bronchial wall thickening (n = 6) but no patients had underlying pulmonary fibrosis [81]. Wang *et al*[82] reported that during days 12-17 there was a notable increase in the mixed pattern, although GGO were still predominant. Xiong *et al*[83] observed that after an average of 11.6 d the follow-up CT showed progressive GGO, consolidation, interstitial thickening, fibrous stripes, and air bronchograms. These findings aid our understanding of the recovery patterns in infected patients. Furthermore, follow-up and management plans will need high-quality evidence to guide clinical decision-making and monitor treatment efficacy with supplemental oxygen and antifibrotic agents.

AI INTERVENTIONAL SYSTEMS

AI is a broad concept that refers to a set of advanced computational algorithms that utilizes heuristic pattern recognition for a given training dataset and therefore makes predictions on unseen testing datasets. Radiomics utilizes data-characterization algorithms for extracting and evaluating features from radiological medical images and further uses them to creating statistical models with the intent to provide support for diagnosis and management[84]. Radiologic parameters considered for analysis include size, shape and textural features that have useful spatial information on pixel or voxel distribution and patterns[85]. Integration of AI into radiomic datasets has the potential to streamline COVID-19 diagnosis. In early February 2020, Beijing-based AI company *Infervision* launched the "Coronavirus artificial intelligence solution," an algorithm that utilizes CT imaging data to diagnose COVID-19 on CT[86]. The reports revealed an increased ability to read images in 10 s, drastically improving clinical workflow efficiency, and reducing variable human error, while continuously improving diagnostic accuracy[87].

Another study developed a deep-learning COVID-19 diagnosis system from a dataset including 11356 CT volumes from COVID-19, influenza-A/B, non-viral community-acquired pneumonia and non-pneumonia subjects from China[88]. The basic workflow of the deep-learning-based diagnosis model contains utilization of CT data as the input, the lung is then segmented, COVID-19 diagnosis is made based on the location of infectious slices (Figure 12). This study found that the AI system outperformed very experienced radiologists based on speed. Another study by Harmon *et al*[89] showed that the use of the AI system that can detect COVID-19 pneumonia with 90.8% accuracy, 84% sensitivity, and 93% specificity. A total of 1280 patients from China, Italy, and Japan were used to train the deep-learning algorithms, and the system was tested independently on 1337 patients, with normal controls from oncology, emergency, and pneumonia-related indications. There was a 10% false-positive rate of incorrectly diagnosed COVID-19 related patients. This indicates potential for overlapped diagnosis with other pneumonia etiologies. Another limiting factor in using AI is the need for thousands of high-quality CT studies to train the AI. Overall, AI systems could be trained to be extremely accurate, sensitive, and specific for COVID-19 diagnosis. However, it may be more useful in specific assessment of imaging findings of COVID-19[88,89].

A subsequent study conducted by Yu *et al*[90] investigated various pre-trained deep learning AI models against 246 severe cases and 483 non-severe COVID-19 cases and found that DenseNet-201 with cubic SVM model achieved a high severity classification accuracy of 95.20% and 95.34% for ten-fold cross-validation and leave-one-out validation, respectively. These effective results show that the utility of the proposed pipeline model was able to achieve a rapid and accurate identification of the severity of COVID-19, indicating its potential for use by clinicians in not just diagnosis but also

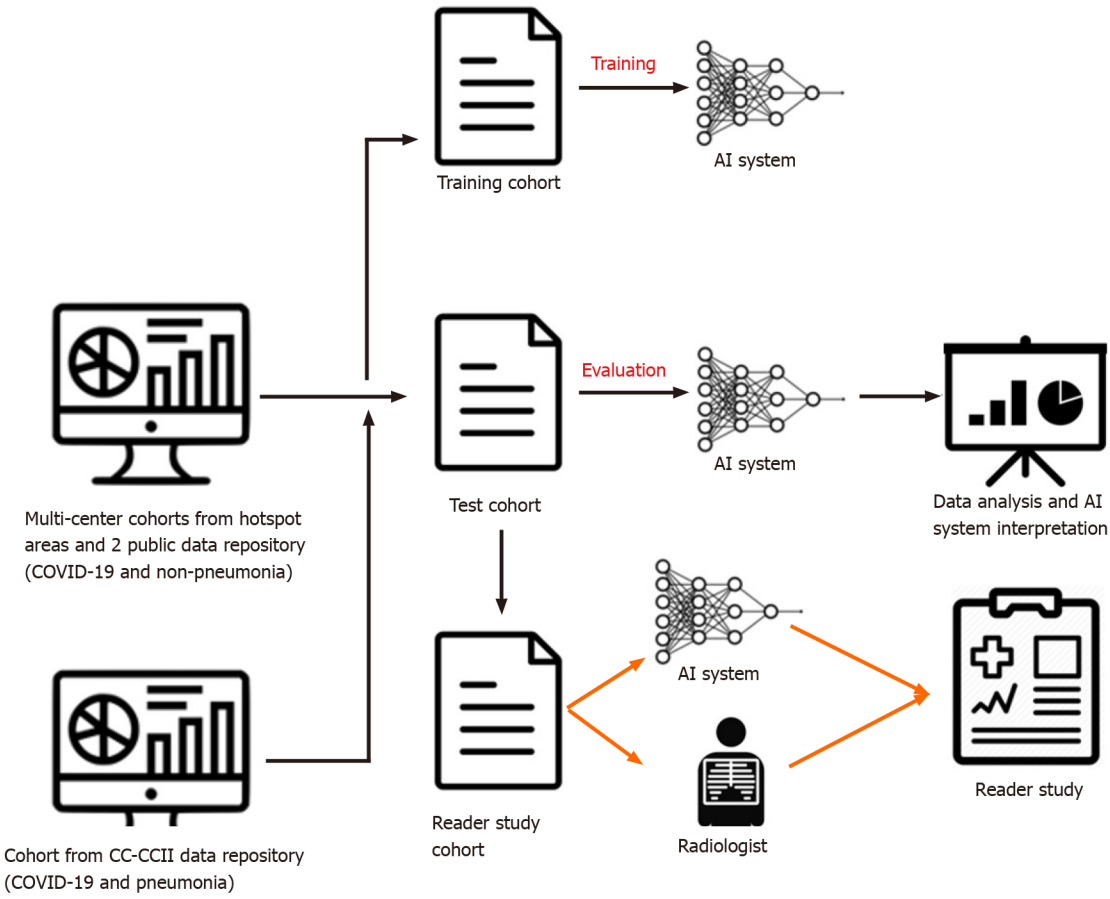

Figure 12 Basic workflow of the artificial intelligence system. AI: Artificial intelligence; COVID-19: Coronavirus disease 2019.

decisions relating to severity management and prioritization[90].

In May 2020, radiologist Laghi[91] wrote a correspondence letter in *The Lancet* detailing her concern that the diagnostic value of AI algorithms in CT scans was not supported by scientific evidence. In fact, since the high-resolution CT findings are not pathognomonic of COVID-19 infection and have poor accuracy in screening asymptomatic individuals according to the American College of Radiology, there have been growing concerns over the integration of AI radiology into the screening of this disease[92].

RADIOLOGY PANEL: FIRST AND SECOND WAVE

First wave experience

The overwhelming nature of COVID-19 has strained global healthcare services and greatly impacted radiology departments. To cope with increasing admissions during peaks, radiologists and radiology trainees have experienced redeployment to areas of clinical need. One hospital saw 21% of their total radiology employees reassigned to other duties[93]. Following official guidelines[94], medical facilities also rescheduled non-urgent elective procedures, and this had a major effect on total imaging volume. While the exact drop varies within institutions, a large New York metropolitan health system reported an 87%, 4%, and 45% reduction in outpatient, inpatient, and emergency imaging respectively, during the pandemic[95].

Moreover, it has become increasingly evident that COVID-19 is not limited to the lungs, rather it can affect other organs too. An early published clinical cohort of COVID-19 displayed acute cardiac injury, shock, and arrhythmia in 7.2%, 8.7%, and 16.7% of patients respectively, with a higher prevalence in patients requiring intensive care[96]. Neurological manifestations have also been recorded; another observational study demonstrated neurological symptoms in 36.4% of hospitalized COVID patients [97]. Alongside observations of kidney involvement and hypercoagulability in patients, this leaves a potentially important role for radiologists when considering

COVID-19 as a multisystem disease[98,99].

Regarding the role of imaging, our understanding has changed with the course of the pandemic. Chest CT was temporarily part of the official diagnostic criteria for COVID-19 due to the nature of the early emergency in China; however, since then, chest CT findings are no longer considered diagnostic. Current guidelines establish that RT-PCR assays are the standard for definitive COVID-19 diagnosis[100,101]. Instead, CXR and chest CT have been the most common imaging modalities specified for presumptive diagnosis, triage and management of patients with suspected or known COVID-19 infection[102]. After the diagnosis is confirmed, the role of imaging may be limited but while waiting for PCR positive it can be very useful for clinicians. Portable CXR is often used as the primary imaging study in suspected patients, chest CT is far more sensitive in detecting lung lesions but has been reserved for more specific cases[4,13].

FORWARD PREPARATION FOR THE SECOND WAVE

As radiologists get ready for the second wave of COVID-19, it is important to continue developing on lessons learned from the 1st wave. With that in mind, a general framework that can be applied to radiology departments when preparing for the second wave and beyond is the concepts of building, sustaining, and adapting[103].

The main idea of the first strategy is to create capacity before it is needed. This can be done by increasing hours of staff, getting more manpower, or by expanding operations into other sites as seen in Singapore General Hospital's (SGH) Emergency Department[103]. When faced with increased local transmission of COVID-19, management of an adjacent Ambulatory Surgery Centre was transferred to the ED, allowing for operations to be ramped up and for portable radiology services to grow [104]. Additional capacity can also be created by increasing portable imaging capability through renting extra units so they can be deployed into operations when needed[105].

Moving on to the second strategy of sustaining, the central idea here is to operate at a pace that is maintainable in the long-term. This would involve preserving supplies such as Personal Protective Equipment, preventing staff burnout, simplifying hastily designed processes, and alternating work times or work sites[103]. In the University of Alabama at Birmingham, home picture archiving and communication system workstations were rapidly deployed in anticipation of a potential COVID-19 crisis [106]. With this measure, the number of people coming on-site could be limited in the long-term while also contributing to social distancing amongst radiologists.

Lastly, the third strategy, adapting, highlights the importance of being flexible. Some ways this can be achieved include rapidly scaling up responses, reconfiguring spaces, improvising, and embracing new roles when faced with increased demands [103]. This is demonstrated at SGH, where in order to monitor changes in the pandemic, a smaller radiology disease outbreak task force was assembled to assess overnight incidents and anticipate changes during the day[4].

CONCLUSION

The burden of this disease is evident through the rampant rise in fatality, morbidity, and mortality rates across the world. Despite the integration of stringent public health measures, this spread continues and is leaving an everlasting impact on both humanity and the economy. Radiologists have significantly adjusted their practices in accordance with the pandemic and as frontline workers, it is essential for them to identify the classical findings associated with COVID-19 and use their expertise towards engaging in optimal strategies to slow disease progression. Advances in the role of radiology in COVID-19 research have piled up within a short-period, hence it is prudent to remain acquainted with important findings. Some notable findings consist of the early stage of disease producing a classical GGO appearance on majority of the CT scans, and the late stage of disease showing highly specific fibrotic lesions due to scarring of the lung parenchyma. The purpose of identifying these characteristic features and associating them with a time course can be crucial towards the management plan for each patient. Additionally, the role of radiology can further be integrated into the scoring systems discussed in this review for risk stratification and appropriate assessment and treatment strategies for infected cases. Nevertheless, medical imaging has been suggested to have promising value as a rapid adjunctive

tool in patients with COVID-19 through assisting with the diagnosis, evaluating patients with clinical deterioration, and providing the multidisciplinary team with vital examinations that could support the management strategies.

REFERENCES

1 **World Health Organization**. Laboratory testing for 2019 novel coronavirus (2019-nCoV) in suspected human cases 19 March 2020. [cited 22 January 2021]. Available from: https://www.who.int/publications/i/item/10665-331501

2 **Böger B**, Fachi MM, Vilhena RO, Cobre AF, Tonin FS, Pontarolo R. Systematic review with meta-analysis of the accuracy of diagnostic tests for COVID-19. *Am J Infect Control* 2021; **49**: 21-29 [PMID: 32659413 DOI: 10.1016/j.ajic.2020.07.011]

3 **Liotti FM**, Menchinelli G, Marchetti S, Posteraro B, Landi F, Sanguinetti M, Cattani P. Assessment of SARS-CoV-2 RNA Test Results Among Patients Who Recovered From COVID-19 With Prior Negative Results. *JAMA Intern Med* 2021; **181**: 702-704 [PMID: 33180119 DOI: 10.1001/jamainternmed.2020.7570]

4 **Mossa-Basha M**, Meltzer CC, Kim DC, Tuite MJ, Kolli KP, Tan BS. Radiology Department Preparedness for COVID-19: *Radiology* Scientific Expert Review Panel. *Radiology* 2020; **296**: E106-E112 [PMID: 32175814 DOI: 10.1148/radiol.2020200988]

5 **Younes N**, Al-Sadeq DW, Al-Jighefee H, Younes S, Al-Jamal O, Daas HI, Yassine HM, Nasrallah GK. Challenges in Laboratory Diagnosis of the Novel Coronavirus SARS-CoV-2. *Viruses* 2020; **12**: 582 [PMID: 32466458 DOI: 10.3390/v12060582]

6 **Weiss SR**, Navas-Martin S. Coronavirus pathogenesis and the emerging pathogen severe acute respiratory syndrome coronavirus. *Microbiol Mol Biol Rev* 2005; **69**: 635-664 [PMID: 16339739 DOI: 10.1128/MMBR.69.4.635-664.2005]

7 **Yuki K**, Fujiogi M, Koutsogiannaki S. COVID-19 pathophysiology: A review. *Clin Immunol* 2020; **215**: 108427 [PMID: 32325252 DOI: 10.1016/j.clim.2020.108427]

8 **Corman VM**, Muth D, Niemeyer D, Drosten C. Chapter Eight - Hosts and Sources of Endemic Human Coronaviruses. In: Advances in Virus Research. Kielian M, Mettenleiter TC, Roossinck MJ, editors. Elsevier, 2018: 163-188 [DOI: 10.1016/bs.aivir.2018.01.001]

9 **Kakodkar P**, Kaka N, Baig MN. A Comprehensive Literature Review on the Clinical Presentation, and Management of the Pandemic Coronavirus Disease 2019 (COVID-19). *Cureus* 2020; **12**: e7560 [PMID: 32269893 DOI: 10.7759/cureus.7560]

10 **Kim EA**, Lee KS, Primack SL, Yoon HK, Byun HS, Kim TS, Suh GY, Kwon OJ, Han J. Viral pneumonias in adults: radiologic and pathologic findings. *Radiographics* 2002; **22**: S137-S149 [PMID: 12376607 DOI: 10.1148/radiographics.22.suppl_1.g02oc15s137]

11 **Luks AM**, Freer L, Grissom CK, McIntosh SE, Schoene RB, Swenson ER, Hackett PH. COVID-19 Lung Injury is Not High Altitude Pulmonary Edema. *High Alt Med Biol* 2020; **21**: 192-193 [PMID: 32281877 DOI: 10.1089/ham.2020.0055]

12 **Gralinski LE**, Baric RS. Molecular pathology of emerging coronavirus infections. *J Pathol* 2015; **235**: 185-195 [PMID: 25270030 DOI: 10.1002/path.4454]

13 **Manna S**, Wruble J, Maron SZ, Toussie D, Voutsinas N, Finkelstein M, Cedillo MA, Diamond J, Eber C, Jacobi A, Chung M, Bernheim A. COVID-19: A Multimodality Review of Radiologic Techniques, Clinical Utility, and Imaging Features. *Radiol Cardiothorac Imaging* 2020; **2**: e200210 [PMID: 33778588 DOI: 10.1148/ryct.2020200210]

14 **Lev MH**, Gonzalez RG. 17 - CT Angiography and CT Perfusion Imaging. In: Brain Mapping: The Methods. 2nd ed. Toga AW, Mazziotta JC, editors. San Diego: Academic Press, 2002: 427-484 [DOI: 10.1016/b978-012088592-3/50076-1]

15 **Singh B**, Kaur P, Reid RJ, Shamoon F, Bikkina M. COVID-19 and Influenza Co-Infection: Report of Three Cases. *Cureus* 2020; **12**: e9852 [PMID: 32832306 DOI: 10.7759/cureus.9852]

16 **Shi H**, Han X, Jiang N, Cao Y, Alwalid O, Gu J, Fan Y, Zheng C. Radiological findings from 81 patients with COVID-19 pneumonia in Wuhan, China: a descriptive study. *Lancet Infect Dis* 2020; **20**: 425-434 [PMID: 32105637 DOI: 10.1016/S1473-3099(20)30086-4]

17 **Pormohammad A**, Ghorbani S, Khatami A, Farzi R, Baradaran B, Turner DL, Turner RJ, Bahr NC, Idrovo JP. Comparison of confirmed COVID-19 with SARS and MERS cases - Clinical characteristics, laboratory findings, radiographic signs and outcomes: A systematic review and meta-analysis. *Rev Med Virol* 2020; **30**: e2112 [PMID: 32502331 DOI: 10.1002/rmv.2112]

18 **Carotti M**, Salaffi F, Sarzi-Puttini P, Agostini A, Borgheresi A, Minorati D, Galli M, Marotto D, Giovagnoni A. Chest CT features of coronavirus disease 2019 (COVID-19) pneumonia: key points for radiologists. *Radiol Med* 2020; **125**: 636-646 [PMID: 32500509 DOI: 10.1007/s11547-020-01237-4]

19 **Martini K**, Blüthgen C, Walter JE, Messerli M, Nguyen-Kim TDL, Frauenfelder T. Accuracy of Conventional and Machine Learning Enhanced Chest Radiography for the Assessment of COVID-19 Pneumonia: Intra-Individual Comparison with CT. *J Clin Med* 2020; **9**: 3576 [PMID: 33171999 DOI: 10.3390/jcm9113576]

20 **Rampa L**, Miceli A, Casilli F, Biraghi T, Barbara B, Donatelli F. Lung complication in COVID-19 convalescence: A spontaneous pneumothorax and pneumatocele case report. *J Respir Dis Med* 2020;

2 [DOI: 10.15761/jrdm.1000115]
21 **Kaufman AE**, Naidu S, Ramachandran S, Kaufman DS, Fayad ZA, Mani V. Review of radiographic findings in COVID-19. *World J Radiol* 2020; **12**: 142-155 [PMID: 32913561 DOI: 10.4329/wjr.v12.i8.142]
22 **Yasin R**, Gouda W. Chest X-ray findings monitoring COVID-19 disease course and severity. *Egypt J Radiol Nucl Med* 2020; **51**: 193 [DOI: 10.1186/s43055-020-00296-x]
23 **Borakati A**, Perera A, Johnson J, Sood T. Diagnostic accuracy of X-ray versus CT in COVID-19: a propensity-matched database study. *BMJ Open* 2020; **10**: e042946 [PMID: 33158840 DOI: 10.1136/bmjopen-2020-042946]
24 **Ng MY**, Lee EYP, Yang J, Yang F, Li X, Wang H, Lui MM, Lo CS, Leung B, Khong PL, Hui CK, Yuen KY, Kuo MD. Imaging Profile of the COVID-19 Infection: Radiologic Findings and Literature Review. *Radiol Cardiothorac Imaging* 2020; **2**: e200034 [PMID: 33778547 DOI: 10.1148/ryct.2020200034]
25 **Bao C**, Liu X, Zhang H, Li Y, Liu J. Coronavirus Disease 2019 (COVID-19) CT Findings: A Systematic Review and Meta-analysis. *J Am Coll Radiol* 2020; **17**: 701-709 [PMID: 32283052 DOI: 10.1016/j.jacr.2020.03.006]
26 **Gillespie M**, Flannery P, Schumann JA, Dincher N, Mills R, Can A. Crazy-Paving: A Computed Tomographic Finding of Coronavirus Disease 2019. *Clin Pract Cases Emerg Med* 2020; **4**: 461-463 [PMID: 32926713 DOI: 10.5811/cpcem.2020.5.47998]
27 **Fu Z**, Tang N, Chen Y, Ma L, Wei Y, Lu Y, Ye K, Liu H, Tang F, Huang G, Yang Y, Xu F. CT features of COVID-19 patients with two consecutive negative RT-PCR tests after treatment. *Sci Rep* 2020; **10**: 11548 [PMID: 32665633 DOI: 10.1038/s41598-020-68509-x]
28 **Ali TF**, Tawab MA, ElHariri MA. CT chest of COVID-19 patients: What should a radiologist know? *Egypt J Radiol Nucl Med* 2020; **51**: 120 [DOI: 10.1186/s43055-020-00245-8]
29 **Pakdemirli E**, Mandalia U, Monib S. Positive Chest CT Features in Patients With COVID-19 Pneumonia and Negative Real-Time Polymerase Chain Reaction Test. *Cureus* 2020; **12**: e9942 [PMID: 32850265 DOI: 10.7759/cureus.9942]
30 **Sales AR**, Casagrande EM, Hochhegger B, Zanetti G, Marchiori E. The Reversed Halo Sign and COVID-19: Possible Histopathological Mechanisms Related to the Appearance of This Imaging Finding. *Arch Bronconeumol* 2021; **57** Suppl 1: 73-75 [PMID: 32792171 DOI: 10.1016/j.arbres.2020.06.029]
31 **Ojha V**, Mani A, Pandey NN, Sharma S, Kumar S. CT in coronavirus disease 2019 (COVID-19): a systematic review of chest CT findings in 4410 adult patients. *Eur Radiol* 2020; **30**: 6129-6138 [PMID: 32474632 DOI: 10.1007/s00330-020-06975-7]
32 **Kwee TC**, Kwee RM. Chest CT in COVID-19: What the Radiologist Needs to Know. *Radiographics* 2020; **40**: 1848-1865 [PMID: 33095680 DOI: 10.1148/rg.2020200159]
33 **Kong W**, Agarwal PP. Chest Imaging Appearance of COVID-19 Infection. *Radiol Cardiothorac Imaging* 2020; **2**: e200028 [PMID: 33778544 DOI: 10.1148/ryct.2020200028]
34 **Meirelles GSP**. COVID-19: a brief update for radiologists. *Radiol Bras* 2020; **53**: 320-328 [PMID: 33071376 DOI: 10.1590/0100-3984.2020.0074]
35 **Zhang Q**, Douglas A, Abideen ZU, Khanal S, Tzarnas S. Novel Coronavirus (2019-nCoV) in Disguise. *Cureus* 2020; **12**: e7521 [PMID: 32377469 DOI: 10.7759/cureus.7521]
36 **Mughal MS**, Rehman R, Osman R, Kan N, Mirza H, Eng MH. Hilar lymphadenopathy, a novel finding in the setting of coronavirus disease (COVID-19): A case report. *J Med Case Rep* 2020; **14**: 124 [PMID: 32771058 DOI: 10.1186/s13256-020-02452-3]
37 **Kovács A**, Palásti P, Veréb D, Bozsik B, Palkó A, Kincses ZT. The sensitivity and specificity of chest CT in the diagnosis of COVID-19. *Eur Radiol* 2021; **31**: 2819-2824 [PMID: 33051732 DOI: 10.1007/s00330-020-07347-x]
38 **Souza CA**, Müller NL, Johkoh T, Akira M. Drug-induced eosinophilic pneumonia: high-resolution CT findings in 14 patients. *AJR Am J Roentgenol* 2006; **186**: 368-373 [PMID: 16423940 DOI: 10.2214/AJR.04.1847]
39 **Rossi SE**, Erasmus JJ, McAdams HP, Sporn TA, Goodman PC. Pulmonary drug toxicity: radiologic and pathologic manifestations. *Radiographics* 2000; **20**: 1245-1259 [PMID: 10992015 DOI: 10.1148/radiographics.20.5.g00se081245]
40 **Lin YH**, Hsu HS. Ground glass opacity on chest CT scans from screening to treatment: A literature review. *J Chin Med Assoc* 2020; **83**: 887-890 [PMID: 32675737 DOI: 10.1097/JCMA.0000000000000394]
41 **Gu J**, Yang L, Li T, Liu Y, Zhang J, Ning K, Su D. Temporal relationship between serial RT-PCR results and serial chest CT imaging, and serial CT changes in coronavirus 2019 (COVID-19) pneumonia: a descriptive study of 155 cases in China. *Eur Radiol* 2021; **31**: 1175-1184 [PMID: 32930834 DOI: 10.1007/s00330-020-07268-9]
42 **Pan F**, Ye T, Sun P, Gui S, Liang B, Li L, Zheng D, Wang J, Hesketh RL, Yang L, Zheng C. Time Course of Lung Changes at Chest CT during Recovery from Coronavirus Disease 2019 (COVID-19). *Radiology* 2020; **295**: 715-721 [PMID: 32053470 DOI: 10.1148/radiol.2020200370]
43 **Peng QY**, Wang XT, Zhang LN; Chinese Critical Care Ultrasound Study Group (CCUSG). Findings of lung ultrasonography of novel corona virus pneumonia during the 2019-2020 epidemic. *Intensive Care Med* 2020; **46**: 849-850 [PMID: 32166346 DOI: 10.1007/s00134-020-05996-6]
44 **Poggiali E**, Dacrema A, Bastoni D, Tinelli V, Demichele E, Mateo Ramos P, Marcianò T, Silva M, Vercelli A, Magnacavallo A. Can Lung US Help Critical Care Clinicians in the Early Diagnosis of

Novel Coronavirus (COVID-19) Pneumonia? *Radiology* 2020; **295**: E6 [PMID: 32167853 DOI: 10.1148/radiol.2020200847]

45 **Via G**, Storti E, Gulati G, Neri L, Mojoli F, Braschi A. Lung ultrasound in the ICU: from diagnostic instrument to respiratory monitoring tool. *Minerva Anestesiol* 2012; **78**: 1282-1296 [PMID: 22858877]

46 **Vetrugno L**, Bove T, Orso D, Barbariol F, Bassi F, Boero E, Ferrari G, Kong R. Our Italian experience using lung ultrasound for identification, grading and serial follow-up of severity of lung involvement for management of patients with COVID-19. *Echocardiography* 2020; **37**: 625-627 [PMID: 32239532 DOI: 10.1111/echo.14664]

47 **Testa A**, Soldati G, Copetti R, Giannuzzi R, Portale G, Gentiloni-Silveri N. Early recognition of the 2009 pandemic influenza A (H1N1) pneumonia by chest ultrasound. *Crit Care* 2012; **16**: R30 [PMID: 22340202 DOI: 10.1186/cc11201]

48 **Bitar ZI**, Maadarani OS, El-Shably AM, Al-Ajmi MJ. Diagnostic accuracy of chest ultrasound in patients with pneumonia in the intensive care unit: A single-hospital study. *Health Sci Rep* 2019; **2**: e102 [PMID: 30697596 DOI: 10.1002/hsr2.102]

49 **Youssef A**, Serra C, Pilu G. Lung ultrasound in the coronavirus disease 2019 pandemic: a practical guide for obstetricians and gynecologists. *Am J Obstet Gynecol* 2020; **223**: 128-131 [PMID: 32437667 DOI: 10.1016/j.ajog.2020.05.014]

50 **Moro F**, Buonsenso D, Moruzzi MC, Inchingolo R, Smargiassi A, Demi L, Larici AR, Scambia G, Lanzone A, Testa AC. How to perform lung ultrasound in pregnant women with suspected COVID-19. *Ultrasound Obstet Gynecol* 2020; **55**: 593-598 [PMID: 32207208 DOI: 10.1002/uog.22028]

51 **Gargani L**, Sicari R, Raciti M, Serasini L, Passera M, Torino C, Letachowicz K, Ekart R, Fliser D, Covic A, Balafa O, Stavroulopoulos A, Massy ZA, Fiaccadori E, Caiazza A, Bachelet T, Slotki I, Shavit L, Martinez-Castelao A, Coudert-Krier MJ, Rossignol P, Kraemer TD, Hannedouche T, Panichi V, Wiecek A, Pontoriero G, Sarafidis P, Klinger M, Hojs R, Seiler-Mußler S, Lizzi F, Onofriescu M, Zarzoulas F, Tripepi R, Mallamaci F, Tripepi G, Picano E, London GM, Zoccali C. Efficacy of a remote web-based lung ultrasound training for nephrologists and cardiologists: a LUST trial sub-project. *Nephrol Dial Transplant* 2016; **31**: 1982-1988 [PMID: 27672089 DOI: 10.1093/ndt/gfw329]

52 **Cardim N**, Dalen H, Voigt JU, Ionescu A, Price S, Neskovic AN, Edvardsen T, Galderisi M, Sicari R, Donal E, Stefanidis A, Delgado V, Zamorano J, Popescu BA. The use of handheld ultrasound devices: a position statement of the European Association of Cardiovascular Imaging (2018 update). *Eur Heart J Cardiovasc Imaging* 2019; **20**: 245-252 [PMID: 30351358 DOI: 10.1093/ehjci/jey145]

53 **News BW**. ICN CEO Howard Catton BBC World News interview on COVID-19. In: Who's Who. Bloomsbury Publishing plc, 2018 [DOI: 10.1093/ww/9780199540884.013.u17734]

54 **Buonsenso D**, Piano A, Raffaelli F, Bonadia N, de Gaetano Donati K, Franceschi F. Point-of-Care Lung Ultrasound findings in novel coronavirus disease-19 pnemoniae: a case report and potential applications during COVID-19 outbreak. *Eur Rev Med Pharmacol Sci* 2020; **24**: 2776-2780 [PMID: 32196627 DOI: 10.26355/eurrev_202003_20549]

55 **Lichtenstein DA**, Mezière GA, Lagoueyte JF, Biderman P, Goldstein I, Gepner A. A-lines and B-lines: lung ultrasound as a bedside tool for predicting pulmonary artery occlusion pressure in the critically ill. *Chest* 2009; **136**: 1014-1020 [PMID: 19809049 DOI: 10.1378/chest.09-0001]

56 **Volpicelli G**, Lamorte A, Villén T. What's new in lung ultrasound during the COVID-19 pandemic. *Intensive Care Med* 2020; **46**: 1445-1448 [PMID: 32367169 DOI: 10.1007/s00134-020-06048-9]

57 **Allinovi M**, Parise A, Giacalone M, Amerio A, Delsante M, Odone A, Franci A, Gigliotti F, Amadasi S, Delmonte D, Parri N, Mangia A. Lung Ultrasound May Support Diagnosis and Monitoring of COVID-19 Pneumonia. *Ultrasound Med Biol* 2020; **46**: 2908-2917 [PMID: 32807570 DOI: 10.1016/j.ultrasmedbio.2020.07.018]

58 **Huang Y**, Wang S, Liu Y, Zhang Y, Zheng C, Zheng Y, Zhang C, Min W, Zhou H, Yu M, Hu M. A preliminary study on the ultrasonic manifestations of peripulmonary lesions of non-critical novel coronavirus pneumonia (COVID-19). *SSRN* 2020 [DOI: 10.2139/ssrn.3544750]

59 **Norbedo S**, Blaivas M, Raffaldi I, Caroselli C. Lung Ultrasound Point-of-View in Pediatric and Adult COVID-19 Infection. *J Ultrasound Med* 2021; **40**: 899-908 [PMID: 32894621 DOI: 10.1002/jum.15475]

60 **McDermott C**, Daly J, Carley S. Combatting COVID-19: is ultrasound an important piece in the diagnostic puzzle? *Emerg Med J* 2020; **37**: 644-649 [PMID: 32907844 DOI: 10.1136/emermed-2020-209721]

61 **Zhu F**, Zhao X, Wang T, Wang Z, Guo F, Xue H, Chang P, Liang H, Ni W, Wang Y, Chen L, Jiang B. Ultrasonic Characteristics and Severity Assessment of Lung Ultrasound in COVID-19 Pneumonia in Wuhan, China: A Retrospective, Observational Study. *Engineering* 2020; **7**: 367-375 [DOI: 10.1016/j.eng.2020.09.007]

62 **Soldati G**, Smargiassi A, Inchingolo R, Buonsenso D, Perrone T, Briganti DF, Perlini S, Torri E, Mariani A, Mossolani EE, Tursi F, Mento F, Demi L. Proposal for International Standardization of the Use of Lung Ultrasound for Patients With COVID-19: A Simple, Quantitative, Reproducible Method. *J Ultrasound Med* 2020; **39**: 1413-1419 [PMID: 32227492 DOI: 10.1002/jum.15285]

63 **Schmid B**, Feuerstein D, Lang CN, Fink K, Steger R, Rieder M, Duerschmied D, Busch HJ, Damjanovic D. Lung ultrasound in the emergency department - a valuable tool in the management of patients presenting with respiratory symptoms during the SARS-CoV-2 pandemic. *BMC Emerg Med* 2020; **20**: 96 [PMID: 33287732 DOI: 10.1186/s12873-020-00389-w]

64 **Dargent A**, Chatelain E, Kreitmann L, Quenot JP, Cour M, Argaud L; COVID-LUS study group. Lung ultrasound score to monitor COVID-19 pneumonia progression in patients with ARDS. *PLoS One* 2020; **15**: e0236312 [PMID: 32692769 DOI: 10.1371/journal.pone.0236312]

65 **Manivel V**, Lesnewski A, Shamim S, Carbonatto G, Govindan T. CLUE: COVID-19 Lung ultrasound in emergency department. *Emerg Med Australas* 2020; **32**: 694-696 [PMID: 32386264 DOI: 10.1111/1742-6723.13546]

66 **Lu X**, Zhang M, Qian A, Tang L, Xu S. Lung ultrasound score in establishing the timing of intubation in COVID-19 interstitial pneumonia: A preliminary retrospective observational study. *PLoS One* 2020; **15**: e0238679 [PMID: 32881950 DOI: 10.1371/journal.pone.0238679]

67 **Speidel V**, Conen A, Gisler V, Fux CA, Haubitz S. Lung Assessment with Point-of-Care Ultrasound in Respiratory Coronavirus Disease (COVID-19): A Prospective Cohort Study. *Ultrasound Med Biol* 2021; **47**: 896-901 [PMID: 33487473 DOI: 10.1016/j.ultrasmedbio.2020.12.021]

68 **Alfuraih AM**. Point of care lung ultrasound in COVID-19: hype or hope? *BJR Open* 2020; **2**: 20200027 [PMID: 33178984 DOI: 10.1259/bjro.20200027]

69 **Prokop M**, van Everdingen W, van Rees Vellinga T, Quarles van Ufford H, Stöger L, Beenen L, Geurts B, Gietema H, Krdzalic J, Schaefer-Prokop C, van Ginneken B, Brink M; COVID-19 Standardized Reporting Working Group of the Dutch Radiological Society. CO-RADS: A Categorical CT Assessment Scheme for Patients Suspected of Having COVID-19-Definition and Evaluation. *Radiology* 2020; **296**: E97-E104 [PMID: 32339082 DOI: 10.1148/radiol.2020201473]

70 **Bellini D**, Panvini N, Rengo M, Vicini S, Lichtner M, Tieghi T, Ippoliti D, Giulio F, Orlando E, Iozzino M, Ciolfi MG, Montechiarello S, d'Ambrosio U, d'Adamo E, Gambaretto C, Panno S, Caldon V, Ambrogi C, Carbone I. Diagnostic accuracy and interobserver variability of CO-RADS in patients with suspected coronavirus disease-2019: a multireader validation study. *Eur Radiol* 2021; **31**: 1932-1940 [PMID: 32968883 DOI: 10.1007/s00330-020-07273-y]

71 **Ma B**, Gong J, Yang Y, Yao X, Deng X, Chen X. Applicability of MuLBSTA scoring system as diagnostic and prognostic role in early warning of severe COVID-19. *Microb Pathog* 2021; **150**: 104706 [PMID: 33347962 DOI: 10.1016/j.micpath.2020.104706]

72 **Ebrahimian S**, Homayounieh F, Rockenbach MABC, Putha P, Raj T, Dayan I, Bizzo BC, Buch V, Wu D, Kim K, Li Q, Digumarthy SR, Kalra MK. Artificial intelligence matches subjective severity assessment of pneumonia for prediction of patient outcome and need for mechanical ventilation: a cohort study. *Sci Rep* 2021; **11**: 858 [PMID: 33441578 DOI: 10.1038/s41598-020-79470-0]

73 **Signoroni A**, Savardi M, Benini S, Adami N, Leonardi R, Gibellini P, Vaccher F, Ravanelli M, Borghesi A, Maroldi R, Farina D. BS-Net: Learning COVID-19 pneumonia severity on a large chest X-ray dataset. *Med Image Anal* 2021; **71**: 102046 [PMID: 33862337 DOI: 10.1016/j.media.2021.102046]

74 **Maroldi R**, Rondi P, Agazzi GM, Ravanelli M, Borghesi A, Farina D. Which role for chest x-ray score in predicting the outcome in COVID-19 pneumonia? *Eur Radiol* 2021; **31**: 4016-4022 [PMID: 33263159 DOI: 10.1007/s00330-020-07504-2]

75 **Zhao YM**, Shang YM, Song WB, Li QQ, Xie H, Xu QF, Jia JL, Li LM, Mao HL, Zhou XM, Luo H, Gao YF, Xu AG. Follow-up study of the pulmonary function and related physiological characteristics of COVID-19 survivors three months after recovery. *EClinicalMedicine* 2020; **25**: 100463 [PMID: 32838236 DOI: 10.1016/j.eclinm.2020.100463]

76 **Duan YN**, Qin J. Pre- and Posttreatment Chest CT Findings: 2019 Novel Coronavirus (2019-nCoV) Pneumonia. *Radiology* 2020; **295**: 21 [PMID: 32049602 DOI: 10.1148/radiol.2020200323]

77 **Shi H**, Han X, Zheng C. Evolution of CT Manifestations in a Patient Recovered from 2019 Novel Coronavirus (2019-nCoV) Pneumonia in Wuhan, China. *Radiology* 2020; **295**: 20 [PMID: 32032497 DOI: 10.1148/radiol.2020200269]

78 **Li M**, Lei P, Zeng B, Li Z, Yu P, Fan B, Wang C, Zhou J, Hu S, Liu H. Coronavirus Disease (COVID-19): Spectrum of CT Findings and Temporal Progression of the Disease. *Acad Radiol* 2020; **27**: 603-608 [PMID: 32204987 DOI: 10.1016/j.acra.2020.03.003]

79 **Wei J**, Xu H, Xiong J, Shen Q, Fan B, Ye C, Dong W, Hu F. 2019 Novel Coronavirus (COVID-19) Pneumonia: Serial Computed Tomography Findings. *Korean J Radiol* 2020; **21**: 501-504 [PMID: 32100486 DOI: 10.3348/kjr.2020.0112]

80 **Pan Y**, Guan H, Zhou S, Wang Y, Li Q, Zhu T, Hu Q, Xia L. Initial CT findings and temporal changes in patients with the novel coronavirus pneumonia (2019-nCoV): a study of 63 patients in Wuhan, China. *Eur Radiol* 2020; **30**: 3306-3309 [PMID: 32055945 DOI: 10.1007/s00330-020-06731-x]

81 **Bernheim A**, Mei X, Huang M, Yang Y, Fayad ZA, Zhang N, Diao K, Lin B, Zhu X, Li K, Li S, Shan H, Jacobi A, Chung M. Chest CT Findings in Coronavirus Disease-19 (COVID-19): Relationship to Duration of Infection. *Radiology* 2020; **295**: 200463 [PMID: 32077789 DOI: 10.1148/radiol.2020200463]

82 **Wang Y**, Dong C, Hu Y, Li C, Ren Q, Zhang X, Shi H, Zhou M. Temporal Changes of CT Findings in 90 Patients with COVID-19 Pneumonia: A Longitudinal Study. *Radiology* 2020; **296**: E55-E64 [PMID: 32191587 DOI: 10.1148/radiol.2020200843]

83 **Xiong Y**, Sun D, Liu Y, Fan Y, Zhao L, Li X, Zhu W. Clinical and High-Resolution CT Features of the COVID-19 Infection: Comparison of the Initial and Follow-up Changes. *Invest Radiol* 2020; **55**: 332-339 [PMID: 32134800 DOI: 10.1097/RLI.0000000000000674]

84 **Tan HB**, Xiong F, Jiang YL, Huang WC, Wang Y, Li HH, You T, Fu TT, Lu R, Peng BW. The study of automatic machine learning base on radiomics of non-focus area in the first chest CT of

different clinical types of COVID-19 pneumonia. *Sci Rep* 2020; **10**: 18926 [PMID: 33144676 DOI: 10.1038/s41598-020-76141-y]

85 **Gillies RJ**, Kinahan PE, Hricak H. Radiomics: Images Are More than Pictures, They Are Data. *Radiology* 2016; **278**: 563-577 [PMID: 26579733 DOI: 10.1148/radiol.2015151169]

86 **Machine learning in RayStation**. Infervision in the Frontlines Against the Coronavirus 2020. [cited 22 January 2021]. Available from: https://www.itnonline.com/content/infervision-frontlines-against-coronavirus

87 **McCall B**. COVID-19 and artificial intelligence: protecting health-care workers and curbing the spread. *Lancet Digit Health* 2020; **2**: e166-e167 [PMID: 32289116 DOI: 10.1016/S2589-7500(20)30054-6]

88 **Jin C**, Chen W, Cao Y, Xu Z, Tan Z, Zhang X, Deng L, Zheng C, Zhou J, Shi H, Feng J. Development and evaluation of an artificial intelligence system for COVID-19 diagnosis. *Nat Commun* 2020; **11**: 5088 [PMID: 33037212 DOI: 10.1038/s41467-020-18685-1]

89 **Harmon SA**, Sanford TH, Xu S, Turkbey EB, Roth H, Xu Z, Yang D, Myronenko A, Anderson V, Amalou A, Blain M, Kassin M, Long D, Varble N, Walker SM, Bagci U, Ierardi AM, Stellato E, Plensich GG, Franceschelli G, Girlando C, Irmici G, Labella D, Hammoud D, Malayeri A, Jones E, Summers RM, Choyke PL, Xu D, Flores M, Tamura K, Obinata H, Mori H, Patella F, Cariati M, Carrafiello G, An P, Wood BJ, Turkbey B. Artificial intelligence for the detection of COVID-19 pneumonia on chest CT using multinational datasets. *Nat Commun* 2020; **11**: 4080 [PMID: 32796848 DOI: 10.1038/s41467-020-17971-2]

90 **Yu Z**, Li X, Sun H, Wang J, Zhao T, Chen H, Ma Y, Zhu S, Xie Z. Rapid identification of COVID-19 severity in CT scans through classification of deep features. *Biomed Eng Online* 2020; **19**: 63 [PMID: 32787937 DOI: 10.1186/s12938-020-00807-x]

91 **Laghi A**. Cautions about radiologic diagnosis of COVID-19 infection driven by artificial intelligence. *Lancet Digit Health* 2020; **2**: e225 [PMID: 32373786 DOI: 10.1016/S2589-7500(20)30079-0]

92 **Bai HX**, Hsieh B, Xiong Z, Halsey K, Choi JW, Tran TML, Pan I, Shi LB, Wang DC, Mei J, Jiang XL, Zeng QH, Egglin TK, Hu PF, Agarwal S, Xie FF, Li S, Healey T, Atalay MK, Liao WH. Performance of Radiologists in Differentiating COVID-19 from Non-COVID-19 Viral Pneumonia at Chest CT. *Radiology* 2020; **296**: E46-E54 [PMID: 32155105 DOI: 10.1148/radiol.2020200823]

93 **Shi J**, Giess CS, Martin T, Lemaire KA, Curley PJ, Bay C, Mayo-Smith WW, Boland GW, Khorasani R. Radiology Workload Changes During the COVID-19 Pandemic: Implications for Staff Redeployment. *Acad Radiol* 2021; **28**: 1-7 [PMID: 33036897 DOI: 10.1016/j.acra.2020.09.008]

94 **American College of Radiology**. ACR COVID-19 Clinical Resources for Radiologists. 2020 [cited 22 January 2021]. Available from: https://www.acr.org/clinical-resources/COVID-19-Radiology-Resources

95 **Naidich JJ**, Boltyenkov A, Wang JJ, Chusid J, Hughes D, Sanelli PC. Impact of the Coronavirus Disease 2019 (COVID-19) Pandemic on Imaging Case Volumes. *J Am Coll Radiol* 2020; **17**: 865-872 [PMID: 32425710 DOI: 10.1016/j.jacr.2020.05.004]

96 **Wang D**, Hu B, Hu C, Zhu F, Liu X, Zhang J, Wang B, Xiang H, Cheng Z, Xiong Y, Zhao Y, Li Y, Wang X, Peng Z. Clinical Characteristics of 138 Hospitalized Patients With 2019 Novel Coronavirus-Infected Pneumonia in Wuhan, China. *JAMA* 2020; **323**: 1061-1069 [PMID: 32031570 DOI: 10.1001/jama.2020.1585]

97 **Mao L**, Jin H, Wang M, Hu Y, Chen S, He Q, Chang J, Hong C, Zhou Y, Wang D, Miao X, Li Y, Hu B. Neurologic Manifestations of Hospitalized Patients With Coronavirus Disease 2019 in Wuhan, China. *JAMA Neurol* 2020; **77**: 683-690 [PMID: 32275288 DOI: 10.1001/jamaneurol.2020.1127]

98 **Ronco C**, Reis T. Kidney involvement in COVID-19 and rationale for extracorporeal therapies. *Nat Rev Nephrol* 2020; **16**: 308-310 [PMID: 32273593 DOI: 10.1038/s41581-020-0284-7]

99 **Tang N**, Li D, Wang X, Sun Z. Abnormal coagulation parameters are associated with poor prognosis in patients with novel coronavirus pneumonia. *J Thromb Haemost* 2020; **18**: 844-847 [PMID: 32073213 DOI: 10.1111/jth.14768]

100 **American College of Radiology**. ACR Recommendations for the use of Chest Radiography and Computed Tomography (CT) for Suspected COVID-19 Infection. 2020 [cited 22 January 2021]. Available from: https://www.acr.org/Advocacy-and-Economics/ACR-Position-Statements/Recommendations-for-Chest-Radiography-and-CT-for-Suspected-COVID19-Infection

101 **Zu ZY**, Jiang MD, Xu PP, Chen W, Ni QQ, Lu GM, Zhang LJ. Coronavirus Disease 2019 (COVID-19): A Perspective from China. *Radiology* 2020; **296**: E15-E25 [PMID: 32083985 DOI: 10.1148/radiol.2020200490]

102 **Panayiotou A**, Rafailidis V, Puttick T, Satchithananda K, Gray A, Sidhu PS. Escalation and de-escalation of the radiology response to COVID-19 in a tertiary hospital in South London: The King's College Hospital experience. *Br J Radiol* 2020; **93**: 20201034 [PMID: 33112652 DOI: 10.1259/bjr.20201034]

103 **Jeffrey S**. Klein M, Bien Soo Tan, MBBS, Lionel Tim-Ee Cheng, MBBS, Marta Heilbrun, MD, Dushyant Sahani, MD. RSNA Hosts Second Webinar on Radiology Surge and Second Surge Preparedness. [cited 22 January 2021]. Available from: https://www.rsna.org/en/news/2020/June/COVID-19-Surge-Preparedness-Part-Two

104 **Quah LJJ**, Tan BKK, Fua TP, Wee CPJ, Lim CS, Nadarajan G, Zakaria ND, Chan SJ, Wan PW, Teo LT, Chua YY, Wong E, Venkataraman A. Reorganising the emergency department to manage

the COVID-19 outbreak. *Int J Emerg Med* 2020; **13**: 32 [PMID: 32552659 DOI: 10.1186/s12245-020-00294-w]

105 **Cheng LT**, Chan LP, Tan BH, Chen RC, Tay KH, Ling ML, Tan BS. Déjà Vu or Jamais Vu? *AJR Am J Roentgenol* 2020; **214**: 1206-1210 [PMID: 32130047 DOI: 10.2214/AJR.20.22927]

106 **Tridandapani S**, Holl G, Canon CL. Rapid Deployment of Home PACS Workstations to Enable Social Distancing in the Coronavirus Disease (COVID-19) Era. *AJR Am J Roentgenol* 2020; **215**: 1351-1353 [PMID: 32432912 DOI: 10.2214/AJR.20.23495]

Published by **Baishideng Publishing Group Inc**
7041 Koll Center Parkway, Suite 160, Pleasanton, CA 94566, USA
Telephone: +1-925-3991568
E-mail: bpgoffice@wjgnet.com
Help Desk: https://www.f6publishing.com/helpdesk
https://www.wjgnet.com